

# Impact of Exogenous Galectin-9 on Human T Cells

## CONTRIBUTION OF THE T CELL RECEPTOR COMPLEX TO ANTIGEN-INDEPENDENT ACTIVATION BUT NOT TO APOPTOSIS INDUCTION\*

Received for publication, April 24, 2015 Published, JBC Papers in Press, May 6, 2015, DOI 10.1074/jbc.M115.661272

Claire Lhuillier,<sup>a,b,c,1</sup> Clément Barjon,<sup>a,b,c,2</sup> Toshiro Niki,<sup>d,e</sup> Aurore Gelin,<sup>b</sup> Françoise Praz,<sup>f,g</sup> Olivier Morales,<sup>h</sup> Sylvie Souquere,<sup>a,i</sup> Mitsuomi Hirashima,<sup>d,e</sup> Ming Wei,<sup>c</sup> Olivier Dellis,<sup>a,j</sup> and Pierre Busson,<sup>a,b,3</sup>

From the <sup>a</sup>Université Paris-Sud, 15 Rue Georges Clémenceau, 91400, Orsay, France, the <sup>b</sup>CNRS, UMR 8126, Institut Gustave Roussy, 114 Rue Edouard Vaillant, 94805 Villejuif Cedex, France, the <sup>c</sup>Cellvax, Ecole Nationale Vétérinaire d'Alfort, 7 Avenue du Général de Gaulle, 94704 Maisons-Alfort Cedex, France, the <sup>d</sup>Department of Immunology and Immunopathology, Faculty of Medicine, Kagawa University, Kagawa 761-0793, Japan, the <sup>e</sup>GalPharma Co., Ltd., Takamatsu, Kagawa 761-0301, Japan, <sup>f</sup>INSERM, UMR-S 938, Centre de Recherche Saint-Antoine, 75012, Paris, France, the <sup>g</sup>Sorbonne Universités, UPMC Université Paris 06, UMR-S 938, Centre de Recherche Saint-Antoine, 75012, Paris, France, <sup>h</sup>CNRS, UMR 8161 Groupe IRCV, Institut de Biologie de Lille, 1 Rue du Pr. Calmette, 59021 Lille, France, <sup>i</sup>UMR 8122, Institut Gustave Roussy, 114 Rue Edouard Vaillant, 94805 Villejuif Cedex, France, and <sup>j</sup>INSERM, UMR-S 757, Bâtiment 440/443, Rue des Adèles, 91405 Orsay, France

**Background:** Signals triggered by galectin-9 in human T cells are poorly understood.

**Results:** Impairment of Lck or T cell receptor-CD3 complex inhibits calcium mobilization and cytokine production but not apoptosis induced by galectin-9.

**Conclusion:** Galectin-9 triggers two independent pathways in T cells, with one mimicking the antigen-specific activation.

**Significance:** We discovered a novel mechanism involved in galectin-9 immunomodulatory effects.

Galectin-9 (gal-9) is a multifunctional  $\beta$ -galactoside-binding lectin, frequently released in the extracellular medium, where it acts as a pleiotropic immune modulator. Despite its overall immunosuppressive effects, a recent study has reported bimodal action of gal-9 on human resting blood T cells with apoptosis occurring in the majority of them, followed by a wave of activation and expansion of Th1 cells in the surviving population. Our knowledge of the signaling events triggered by exogenous gal-9 in T cells remains limited. One of these events is cytosolic calcium ( $\text{Ca}^{2+}$ ) release reported in some murine and human T cells. The aim of this study was to investigate the contribution of  $\text{Ca}^{2+}$  mobilization to apoptotic and nonapoptotic effects of exogenous gal-9 in human T cells. We found that the T cell receptor (TCR)-CD3 complex and the Lck kinase were required for  $\text{Ca}^{2+}$  mobilization but not for apoptosis induction in Jurkat cells. These data were confirmed in human  $\text{CD4}^+$  T cells from peripheral blood as follows: a specific Lck chemical inhibitor abrogated  $\text{Ca}^{2+}$  mobilization but not apoptosis induction. Moreover, Lck activity was also required for the production of Th1-type cytokines, *i.e.* interleukin-2 and interferon- $\gamma$ , which resulted from gal-9 stimulation in peripheral  $\text{CD4}^+$  T cells. These findings indicate that gal-9 acts on T cells by two distinct pathways as follows: one mimicking antigen-specific activation of the TCR with a mandatory contribution of proximal elements

of the TCR complex, especially Lck, and another resulting in apoptosis that is independent of this complex.

Galectins comprise a family of animal proteins defined by their binding specificity for  $\beta$ -galactosides, in other words disaccharides containing a  $\beta$ 1–3 or  $\beta$ 1–4 galactosyl bond. Most often, these disaccharides are part of complex glycans carried by glycoproteins or glycolipids (1). The domains of galectins that directly interact with carbohydrate ligands are carbohydrate recognition domains (CRD)<sup>4</sup> (2). The CRDs are made of about 135 amino acids forming a groove in which the carbohydrate ligand can bind. Galectin-9 (gal-9) belongs to the category of “tandem repeat” galectins containing two CRDs with distinct specificity linked by a flexible peptide chain called the “linker peptide” (three other human tandem repeat galectins are galectin-4, -8, and -12). As a result of alternative splicing, gal-9 exists in three isoforms characterized by the length of the linker peptide as follows: long, medium (also called  $\Delta$ 5), and short (also called  $\Delta$ 5/6) (3). In basal physiological conditions, gal-9 is weakly expressed in most tissues (with the greatest abundance in the thymus and kidney). Its expression increases in many cell types, including endothelial and epithelial cells, under the influence of the cytokines of the Th1 immune response, especially interferon  $\gamma$  (IFN $\gamma$ ).

Gal-9 is distributed in several cell compartments. A fraction of about 50% is recovered with the soluble elements of the cytoplasm. Another fraction of gal-9 co-purifies with the cellular

\* This work was supported in part by Institut National du Cancer Grant INCADHOS 2010 and the Ligue Nationale Contre le Cancer (Comité du Val de Marne). The authors declare that they have no conflicts of interest with the contents of this article.

<sup>1</sup> Supported by a fellowship from the Association Nationale Recherche-Technologie.

<sup>2</sup> Supported by a fellowship from Association pour la Recherche Contre le Cancer.

<sup>3</sup> To whom correspondence should be addressed. E-mail: pierre.busson@gustaveroussy.fr.

<sup>4</sup> The abbreviations used are: CRD, carbohydrate recognition domain; gal-9, galectin-9; TCR, T cell receptor; PBMC, peripheral blood mononuclear cell; PI, propidium iodide; PHA, phytohemagglutinin; TG, thapsigargin; ANOVA, analysis of variance; PMA, phorbol 12-myristate 13-acetate; ER, endoplasmic reticulum; STR, short tandem repeat; TBP, TATA box-binding protein.

## TCR Complex Signaling and Galectin-9 in Human T Cells

membrane network. Gal-9 is sometimes detected at the surface of the plasma membrane. Finally, a fraction of gal-9 can be detected in the nucleus (4).<sup>5</sup> Like other galectins, gal-9 has no signal sequence. However, it can be secreted by unconventional pathways. We have shown that it is often secreted in association with nanovesicles called exosomes (5, 6). Conversely, Oomizu *et al.* (7) have recently shown that gal-9 is secreted in a soluble form by CD4<sup>+</sup> T cells having surface expression of gal-9 according to a mechanism that remains elusive. Distinct functions have been assigned to intracellular, cell surface, and extracellular gal-9, respectively (3). Cell surface gal-9 plays a role in contacts with neighboring cells and adhesion with extracellular matrix and can activate signaling cascades (8). Secreted extracellular gal-9 either soluble or bound to exosomes often behaves like a cytokine. There are consistent and convergent data from murine experimental systems supporting the notion of an overall immunosuppressive action of gal-9 at the systemic level. These immunosuppressive effects have been demonstrated using models of viral infections, autoimmune diseases, and allogeneic grafts (9–12).

At the cellular level, the phenotypic changes induced by extracellular gal-9 are quite diverse. For a long time, several authors have opposed the inhibitory effects of gal-9 on T cells to the pro-inflammatory effects on cells of the innate immune system, especially NK cells and monocytes (13). However, this perspective has been changed because of more recent findings (14). Using human peripheral blood mononuclear cells (PBMCs), Gooden *et al.* (14) have shown that gal-9 triggers a wave of apoptosis in T cells, which is followed 2–3 days later by a wave of antigen-independent activation in the fraction of surviving cells. It results in the expansion of CD4<sup>+</sup> FoxP3<sup>-</sup> cells, which display mild expression of CD25 as well as IFN $\gamma$  and interleukin-2 (IL-2) production (14). Besides, in the past 4 years, extracellular gal-9 has emerged as a key regulator of adaptive regulatory T cells (T regs) in the human as well as in murine context. gal-9 is a paracrine and/or autocrine factor, which enhances the expansion and the suppressive phenotype of induced regulatory T cells (7, 14–18).

Facing the wide range of phenotypic changes induced by gal-9 in various types of target cells, our knowledge of underlying signaling events remains limited. First, there are controversies about the putative receptors of gal-9 at the surface of the plasma membranes. Initially, gal-9 has been identified as the main agonist of the Tim-3 receptor (19). However, in the past few years, this point has been the subject of controversies (20–22). There is strong evidence that gal-9 is an agonist of Tim-3 in some circumstances, but it is obvious that gal-9 has other membrane receptors, for example the enzyme “disulfide isomerase,” the CD137, or CD44 molecule (18, 23–25). In brief, gal-9 is likely to have several types of membrane receptors and to interact with various combinations of receptors depending on the type of target cells. The intracellular signals generated by these receptors or combinations of receptors remain largely unknown. However, calcium mobilization appears as one of the most consistent signaling events triggered by gal-9 in human

and murine T cells (19, 26, 27). Initially, our aim was to investigate the relationships of calcium mobilization with apoptotic and nonapoptotic events in human T cells stimulated by exogenous gal-9. We observed that in Jurkat cells, calcium mobilization induced by gal-9, but not apoptosis, was dependent on the presence of several elements of the T cell receptor (TCR) complex, including the tyrosine kinase Lck. We then found a critical role of Lck not only in calcium mobilization but also in the induction of the Th1 cytokines IL-2 and IFN $\gamma$ . Finally, similar findings were extended to peripheral blood CD4<sup>+</sup> T cells.

### Experimental Procedures

**Chemicals and Reagents**—The recombinant short isoform of human gal-9 was produced as described previously (28). Recombinant human galectin-8 was purchased commercially (R&D Systems). Lactose ( $\beta$ -lactose) and the synthetic compound A-770041 (a selective Lck inhibitor) were from Sigma and Axon Medchem, respectively.

**Cell Lines**—Human T cell lines (Jurkat E6.1 and MOLT-4) and myeloid cell lines (K562 and THP1) were obtained from American Type Culture Collection. The Lck-deficient Jurkat subline JCaM1.6 and the JCaM1.6/Lck<sup>+</sup> cells (JCaM1.6 stably transfected with the Lck gene) were kindly provided by Dr. Franck Gesbert (Institut Curie, Orsay, France) and Dr. Arthur Weiss (San Francisco) (29). A Jurkat subline knocked down for the CD3  $\zeta$ -chain (by stable transfection of a plasmid encoding a short interfering RNA; CD3 $\zeta$ <sup>-</sup>) and the corresponding “back-in” clone (CD3 $\zeta$ <sup>+</sup>) obtained by stable transfection of an exogenous CD3 $\zeta$  gene were produced, described, and kindly provided by Dr. Richard Proust and Dr. Franck Gesbert (Institut Curie, Orsay, France) (30). The mutant Jurkat subline J31.13 defective for TCR-CD3 surface expression (due to the lack of the TCR  $\beta$ -chain transcript) and the J31.13/TCR $\beta$ <sup>+</sup> cells (stably transfected with an exogenous TCR  $\beta$ -chain gene) were gifts from Dr. Georges Bismuth (Institut Cochin, Paris, France) and Dr. Andres Alcover (Institut Pasteur, Paris, France) (31, 32). All cell lines were grown in RPMI 1640 medium (Gibco, Life Technologies, Inc.) supplemented with 10% fetal calf serum (FCS) at 37 °C in a 5% CO<sub>2</sub>-humidified atmosphere. To maintain a selective pressure on the different Jurkat derivative sublines, the following antibiotics were added: 100  $\mu$ g/ml hygromycin B for JCaM1.6/Lck<sup>+</sup>, 0.5  $\mu$ g/ml puromycin for CD3 $\zeta$ <sup>-</sup>, 5  $\mu$ g/ml blasticidin for CD3 $\zeta$ <sup>+</sup>, and 250  $\mu$ g/ml G418 for 31.13/TCR $\beta$ <sup>+</sup> cell cultures. HeLa cells were cultured in DMEM (Gibco, Life Technologies, Inc.) supplemented with 10% FCS and transiently transfected with plasmids coding for one of the three following genes: GFP and human or murine Tim-3. The TurboFect reagent (ThermoScientific) was used for transfection according to the manufacturer's instructions.

**Genomic DNA Extraction and STR Analysis**—For fingerprint experiments, genomic DNA was isolated from cell pellets using the GeneJET Genomic DNA purification kit (Thermo Scientific) according to the manufacturer's protocol. STR genotypes have been established using the eight highly polymorphic tetranucleotide STR markers recommended by the ATCC (D5S818, D7S820, D13S317, D16S539, CSF1PO, TH01, TPOX, and vWA) and the *Amelogenin* marker that discriminates the X from the Y chromosome that carries a 6-bp insertion. After

<sup>5</sup> P. Busson, unpublished data.

amplification by PCR and capillary electrophoresis, the apparent sizes of the alleles were analyzed using the GeneMapper Analysis 4.0 software (PE Applied Biosystems) as described previously (33).

**Isolation and Culture of PBMCs**—Human PBMCs were obtained from anonymous healthy blood donors using standard density gradient centrifugation (lymphocyte separation medium, Eurobio AbCys) and cultured at 37 °C with 5% CO<sub>2</sub> in RPMI 1640 medium supplemented with 10% FCS. For T cell activation, PBMCs were cultured in anti-CD3 monoclonal antibody (mAb)-coated plates (0.5 μg/ml in PBS) in the presence of soluble anti-CD28 mAb (0.5 μg/ml; both antibodies from Miltenyi Biotec) for 48 h.

**CD4 T Cell Separation**—Untouched CD4 T cells were purified by negative selection using a human CD4<sup>+</sup> T cell isolation kit (Miltenyi Biotec), according to the manufacturer's instructions.

**Apoptosis Assessment**—Human cell lines were treated for 24 h with the indicated concentrations of gal-9 (or gal-8) in serum-free medium (hybridoma-SFM, Gibco). After washing, cells were resuspended in annexin-V-binding buffer and stained with annexin-V-APC (Affymetrix eBioscience) for 15 min in the dark at room temperature. Then propidium iodide (PI) (Sigma) was added to the cell suspension prior to the analysis by flow cytometry (Accuri<sup>®</sup> BD Biosciences). For assessment of CD4<sup>+</sup> T cells apoptosis, PBMCs were treated for 24 h with gal-9 (30 nM) or gal-9 preincubated for 30 min with β-lactose (5 mM), in complete RPMI medium. After washing, PBMCs were stained with anti-human CD4-APC antibody and annexin-V-FITC (BioLegend), followed by PI staining and flow cytometry analysis.

**Caspase Activity Measurement**—Caspase-3 and -7 activities were detected using the Caspase-Glo<sup>®</sup> 3/7 luminescent assay (Promega) according to the manufacturer's protocol. Briefly, the Caspase-Glo 3/7 substrate (Ac-DEVD-*p*-nitroanilide) was cleaved by activated caspases present in the cell protein extracts to release a luciferase substrate. Then the luminescence of each sample was measured at 485/527 nm using a Microlumet LB 96P luminometer (EG&G Berthold). The apoptosis-inducing agent staurosporine (Calbiochem) was used as positive control for caspase activation in this assay.

**Measurement of Cytosolic Calcium Concentration ([Ca<sup>2+</sup>]<sub>cyt</sub>)**—For human cell lines, [Ca<sup>2+</sup>]<sub>cyt</sub> was recorded by a fluorimetric ratio technique (34). Cells were centrifuged and resuspended in Hepes-buffered saline (HBS) medium of the following composition (in mM): 135 NaCl, 5.9 KCl, 1.2 MgCl<sub>2</sub>, 1 CaCl<sub>2</sub>, 11.6 Hepes, 11.5 glucose, pH 7.3, adjusted with NaOH. The fluorescent indicator Indo-1 (4 μM; Invitrogen/Molecular Probes) was loaded by incubating the cells at room temperature under gentle agitation. Cells were then resuspended in HBS medium except in the experiment of Fig. 2D, where cells were resuspended in Ca<sup>2+</sup>-free HBS medium. One million cells were placed in a 1-cm wide, 3-ml quartz cuvette and inserted in a spectrofluorimeter (Varian Cary Eclipse), equipped with a thermostated cuvette holder. Excitation of Indo-1 was done at 360 nm, and emissions at 405 and 480 nm were recorded. Background and autofluorescence were subtracted from the values measured at 405 and 480 nm. Intracellular Ca<sup>2+</sup> concentrations

were calculated following the method already described by Delis and co-workers (34). Traces were given without S.E. for clarity. S.E. values were usually <40 nM. For CD4<sup>+</sup> T cell experiments, [Ca<sup>2+</sup>]<sub>cyt</sub> was recorded by flow cytometry. Briefly, resting PBMCs were stained for CD4 and then incubated at room temperature with 1 μM of the fluorescent indicator Fluo4-AM (Invitrogen). After washing, cells were resuspended in Krebs solution, and cell samples were acquired on the flow cytometer. After gating on CD4<sup>+</sup> T cells, Fluo4-AM fluorescence was recorded continuously following addition of gal-9.

**Western Blot Analysis**—Cell pellets were solubilized in RIPA buffer (150 mM NaCl, 50 mM Tris-HCl, pH 7.4, 5 mM EDTA, 0.5% sodium deoxycholate, 0.5% Nonidet P-40, 0.1% SDS) supplemented with the complete protease inhibitor mixture (Roche Applied Science) and a phosphatase inhibitor mixture (20 mM NaF, 1 mM Na<sub>3</sub>VO<sub>4</sub>, 30 mM β-glycerophosphate, 20 mM Na<sub>4</sub>P<sub>2</sub>O<sub>7</sub>) and sonicated on ice. Extracts were clarified, and protein concentration was determined by the Bradford method using the protein assay from Bio-Rad. Total proteins were separated by SDS-PAGE and transferred to PVDF membranes (Immobilon-P; Millipore) followed by standard Western blotting procedures. The following primary antibodies were used: human Tim-3 antibody (R&D Systems); phospho-Src family (Tyr-416; clone D49G4) rabbit mAb; phospho-Lck (Tyr-505) antibody; Lck (clone 73A5) rabbit mAb (Cell Signaling Technology); CD3-ζ (clone 6B10.2) mouse mAb (Santa Cruz Biotechnology); and β-actin (clone AC-74; Sigma). The anti-pY416 antibody reacts with the activated form of several Src family kinases, including Lck. However, in Jurkat cells it reacts exclusively with Lck as shown by Nika *et al.* (35). Detection was performed using peroxidase-conjugated secondary antibodies and the Immobilon Western Chemiluminescent HRP Substrate (Millipore). Specific protein bands were quantified using the Quantity One software (Bio-Rad).

**Cell-surface Staining**—Wild-type Jurkat and derivative sublines were collected by centrifugation and washed once in PBS prior to staining with an anti-human TCR Vβ8-PE antibody, an anti-human CD3-APC antibody, or a mouse control isotype (BioLegend). After washing, samples were analyzed on the Accuri<sup>®</sup> C6 flow cytometer (BD Biosciences).

**RNA Extraction and RT-PCR**—Total RNA was extracted from Jurkat cells (and derivatives) and isolated CD4<sup>+</sup> T cells using the TRI Reagent solution (MRC gene) and the RNeasy<sup>®</sup> micro kit (Qiagen), respectively, according to the manufacturer's protocols. The cDNA synthesis was performed using the Multiscribe reverse transcriptase (Applied Biosystems). Relative gene expression was determined by quantitative real time PCR using the TaqMan<sup>®</sup> universal Master Mix II and the TaqMan<sup>®</sup> primer/probe sets for human IL-2 (assay ID: Hs00174114\_m1), IFNγ (assay ID: Hs00989291\_m1), and TBP (assay ID: Hs00427620\_m1) (Applied Biosystems). All samples were carried out in duplicate 20- μl reactions in a MicroAmp Optical 96-well reaction plate (Applied Biosystems), and a negative control with no cDNA template was included in every run. The reaction was conducted in the StepOnePlus<sup>™</sup> real time PCR system (Applied Biosystems) with amplification under the following conditions: 95 °C for 10 min, 40 cycles of 95 °C for 15 s and 60 °C for 1 min. The relative expression of the gene was

## TCR Complex Signaling and Galectin-9 in Human T Cells

then determined with the  $2^{-\Delta\Delta Ct}$  (threshold cycle) method, with TBP as an internal control.

**ELISA**—Supernatants from Jurkat and JCaM1.6 cells were collected after 24 h of cell treatment, and the IL-2 concentrations were quantified using a Quantikine Human IL-2 Immunoassay (R&D Systems). Absorbance was measured at 450 nm using a Victor3 plate reader (PerkinElmer Life Sciences).

**Intracellular Cytokine Staining**—After 5 days of culture with the indicated treatments, PBMCs were restimulated with 50 ng/ml phorbol 12-myristate 13-acetate (PMA) and 500 ng/ml ionomycin (Santa Cruz Biotechnology) in the presence of 10  $\mu$ g/ml brefeldin A (Sigma) for 4 h. Cells were washed and stained with anti-human CD3-APC antibody. The cells were then fixed, permeabilized, and stained with anti-human IL-2-FITC and anti-human IFN $\gamma$ -PE antibodies (all antibodies were from BioLegend).

**Statistics**—Data were analyzed using statistical tests (GraphPad Prism 5 software) as explained in the figure legends.

### Results

**Induction of Apoptosis by Exogenous gal-9 in Human T Cell Lines**—Gal-9 induction of apoptosis in Jurkat and MOLT-4 cells has been reported in several studies (26, 27, 36). However, since these publications, induction of apoptosis has also been reported for other cell types by investigators using serum-free media (37). Therefore, we wanted to document the specificity of gal-9-induced apoptosis in T cells. As shown in Fig. 1A, after incubation of Jurkat and MOLT-4 cells with gal-9 (60 nM) for 24 h in serum-free medium, the fraction of apoptotic cells (annexin-V-positive) was substantially increased (up to 70%). In contrast, the fraction of apoptotic cells remained below 15% for the K562 and THP1 cell lines. This result was in favor of a specific pro-apoptotic effect of gal-9 against lymphoid T cell lines. This point was confirmed when we investigated the induction of apoptosis by gal-9, in parallel with gal-8, another tandem repeat galectin with various immunomodulatory effects (Fig. 1B) (38). Using increasing concentrations of gal-9 or gal-8, we observed a dose-dependent induction of apoptosis in Jurkat and MOLT-4 cells only after gal-9 treatment. Again, K562 and THP1 cells were only marginally affected at the highest concentration (60 nM). Gal-9-induced apoptosis was confirmed in Jurkat cells by measuring the activation of the effector caspases (*i.e.* caspase-3 and -7). After 24 h of gal-9 treatment, caspases-3/7 were activated in a dose-dependent manner (Fig. 1C). Moreover, caspase activity was inversely correlated to cell viability (assessed by flow cytometry). At the highest concentration of gal-9 (120 nM), caspase activity was increased almost 10-fold compared with untreated cells and was comparable with caspase activity measured in cells treated with staurosporine (a well known inducer of apoptosis). However, even with substantial concentrations of gal-9, a fraction of Jurkat or MOLT-4 cells resisted apoptosis. Finally, because it has been reported in a murine system that CD4<sup>+</sup> T cell apoptosis induced by gal-9 depends on Tim-3, we investigated the expression of this protein in the lymphoid T cell lines. Tim-3 protein was undetectable in Jurkat and MOLT-4 cells, even after stimulation with PMA (Fig. 1D). In contrast, in HeLa cells transfected with a plasmid coding for the human Tim-3, a high

amount of protein was detected. Thus, gal-9-induced apoptosis is specific for lymphoid T cell lines and does not necessarily involve the Tim-3 receptor.

**Induction of Early Calcium Mobilization by Exogenous gal-9 in Human T Cell Lines**—Gal-9 induction of calcium mobilization has been reported in murine T cells as well as in Jurkat and MOLT-4 human T cells (19, 26, 27). Again, we wanted to further document the specificity of this process. Using the same cell lines previously used for apoptosis assays and the free calcium probe Indo-1, cytosolic calcium concentration ( $[Ca^{2+}]_{cyt}$ ) was assessed following stimulation by recombinant gal-9. Calcium mobilization was readily detected in Jurkat and MOLT-4 cells treated with gal-9, but not in THP1 or K562 cells (Fig. 2A). In contrast, no calcium mobilization was observed in Jurkat cells treated with gal-8 (Fig. 2B). Pretreatment with gal-8 did not impair the gal-9 calcium mobilization (Fig. 2B). The increase in  $[Ca^{2+}]_{cyt}$  induced by gal-9 was dose-dependent with a maximum effect at 45 nM, although an effect was still visible with a concentration as low as 6 nM (Fig. 2C). The effect on  $[Ca^{2+}]_{cyt}$  was rapid, occurring within 30 s after addition of gal-9, and was totally abolished by preincubation with 5 mM lactose (Fig. 2C). In an effort to characterize the pathways of the  $[Ca^{2+}]_{cyt}$  increase, we compared the effect of gal-9 with the effect of thapsigargin (TG) or phytohemagglutinin (PHA). TG is an inhibitor of the sarco/endoplasmic reticulum  $Ca^{2+}$ -ATPases; it allows the release of  $Ca^{2+}$  ions by the endoplasmic reticulum (ER) and the subsequent opening of plasma membrane-specific  $Ca^{2+}$  channels responsible for the store-operated calcium entry. As shown in Fig. 2D, in the absence of extracellular  $Ca^{2+}$  ions, TG induced a slight increase in  $[Ca^{2+}]_{cyt}$  reflecting  $Ca^{2+}$  release from the ER. At the next stage of the experiment, re-addition of extracellular  $Ca^{2+}$  ions (at  $t = 400$  s) resulted in their massive entry reflected by a steep and large increase in  $[Ca^{2+}]_{cyt}$  (not observed in the absence of TG treatment; data not shown). When Jurkat cells were stimulated by 30 nM gal-9, the same sequence (ER  $Ca^{2+}$  release and entry through the store-operated channels) was observed (Fig. 2D). The secondary entry through plasma membrane was inhibited by 30  $\mu$ M 2-aminoethoxydiphenyl borate, an inhibitor of the store-operated calcium entry (Fig. 2D). These data suggested that gal-9 was activating the same  $Ca^{2+}$  pathways as TG. In a subsequent experiment, Jurkat cells were stimulated by PHA in the presence of extracellular  $Ca^{2+}$  ions. PHA is known to cross-link the TCR triggering the activity of the Src family tyrosine kinases, allowing the release of  $Ca^{2+}$  ions from the ER to the cytosol and their subsequent entry from the extracellular medium through the store-operated channels (39). As shown in Fig. 2E, PHA and gal-9 induced similar  $[Ca^{2+}]_{cyt}$  rises. These results suggested that gal-9 was triggering signaling events mimicking the  $Ca^{2+}$  transduction pathway usually activated downstream from the TCR.

**Early Calcium Mobilization but Not Apoptosis Induced by gal-9 Is Dependent on Lck**—Because calcium mobilization induced in Jurkat cells by gal-9 and PHA had the same signature, we hypothesized a contribution of Lck, a tyrosine kinase involved in T cell signaling, in this gal-9 effect. To address this hypothesis, we used a Jurkat mutant subline with selective impairment of Lck (JCaM1.6) (29, 40). As shown in Fig. 3A,

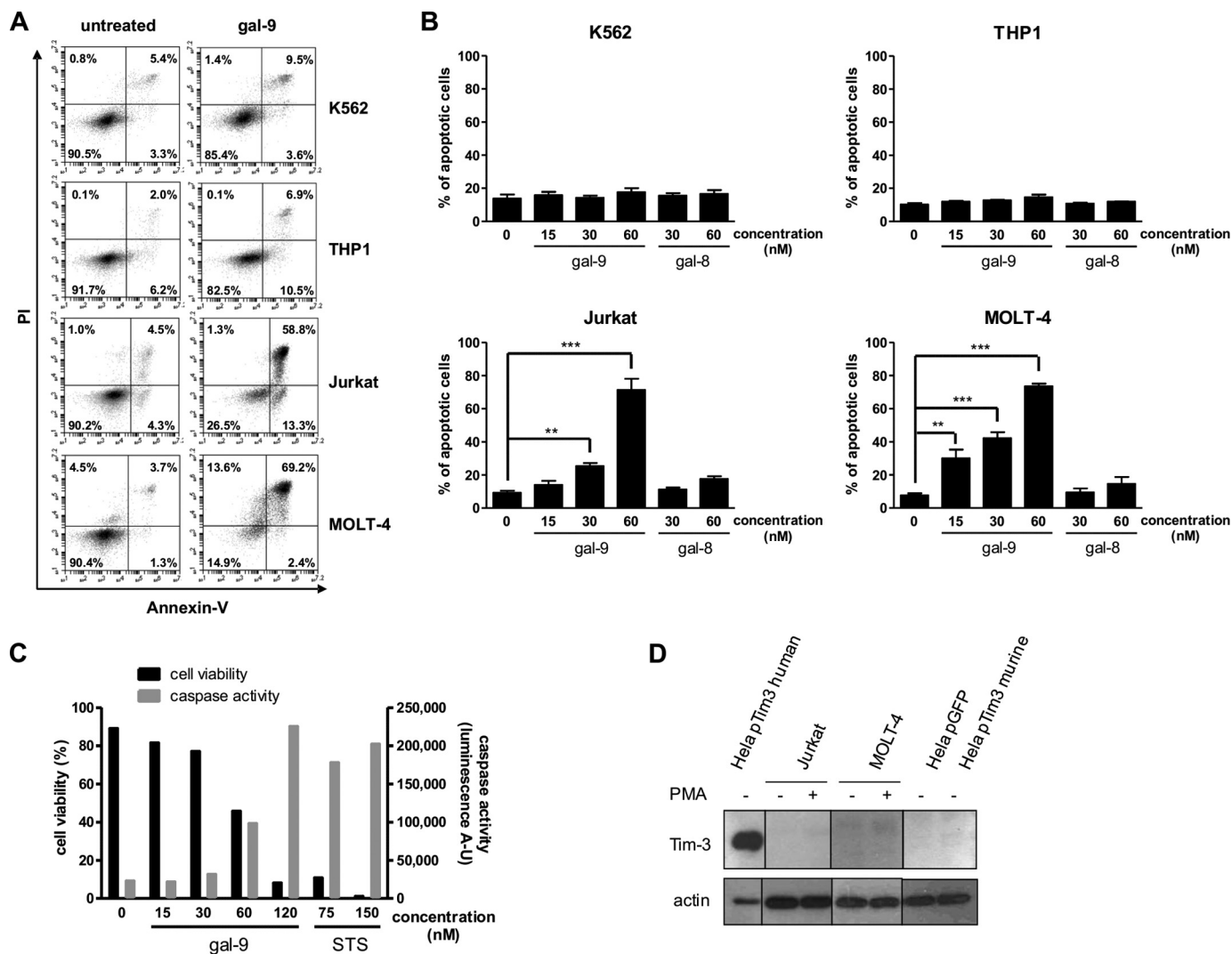


**FIGURE 1. Differential induction of apoptosis by gal-9 in lymphoid T cells and myeloid cells.** *A* and *B*, two myeloid (K562 and THP1) and two lymphoid (Jurkat and MOLT-4) cell lines were treated with various amounts of recombinant gal-9 or gal-8 in serum-free medium for 24 h. Treated cells were stained with annexin-V/PI and then analyzed by flow cytometry. *A*, one example of flow cytometry plots for untreated cells (*left panels*) or cells treated with gal-9 (60 nM; *right panels*) following staining with annexin-V and PI. *Bottom right* quadrants are representative of early apoptotic cells (annexin-V-positive only) and *top right* quadrants of late apoptotic cells (annexin-V- and PI-positive). *B*, comparison of the percentages of apoptotic cells in the four lymphoid and myeloid cell lines treated with recombinant gal-9 or gal-8. Apoptotic cells were counted by flow cytometry as in *A*, taking into account all annexin-V-positive cells. Data are presented as means  $\pm$  S.E. of three independent experiments. \*\*,  $p < 0.01$ ; \*\*\*,  $p < 0.001$ , one-way ANOVA followed by Dunnett's post hoc test. *C*, simultaneous measurement of cell viability and caspase-3/7 activity in Jurkat cells treated with increasing concentrations of gal-9 (0 to 120 nM) or staurosporine (STS; 75 or 150 nM). Following 24 h of treatment, cells were subjected to apoptosis measurement using two assays in parallel, annexin-V/PI staining and a caspase-3/7 enzymatic assay. The percentage of annexin-V-negative cells is represented on the *left y axis* (cell viability). Values of light emission (luminescence arbitrary units (A-U)) are plotted on the *right y axis* and are proportional to the level of activated caspase-3 and -7. The luminescence background value was measured using culture medium without cells. It was at  $63 \pm 5$ . *D*, Jurkat and MOLT-4 cells were treated or not with PMA for 24 h before Tim-3 expression analysis by Western blot. HeLa cells transiently transfected either with a control plasmid coding for GFP (*pGFP*) or a plasmid coding for human Tim-3 (*pTim3 human*) or murine Tim-3 (*pTim3 murine*) were used as positive and negative controls respectively, as the anti-Tim-3 antibody reacts against the human protein only. Actin protein levels were used as loading controls.

calcium mobilization under gal-9 stimulation was abrogated in JCaM1.6 cells indicating that Lck was required for this process. In contrast, calcium mobilization induced by TG was almost identical in JCaM1.6 and Jurkat cells, clearly demonstrating that the  $Ca^{2+}$  machinery was intact in the mutant cell line and that the defect in the response to gal-9 was upstream from the ER  $Ca^{2+}$  release. Therefore, Lck seemed important for the gal-9 transduction pathway. To confirm this observation by an independent approach, we applied a chemical inhibitor of Lck, A-770041, on wild-type (WT) Jurkat cells (41). This chemical compound is 300-fold more selective against Lck ( $IC_{50} = 147$  nM) than against Fyn ( $IC_{50} = 44.1 \mu M$ ), another Src family tyro-

sine kinase involved in T cell signaling (41). As expected, the calcium influx induced by gal-9 was markedly reduced by increasing concentrations of Lck inhibitor and was totally abolished with 170 nM (Fig. 3*B*).

The phosphorylation status of Lck tyrosines is critical for the events linking TCR binding to downstream signaling events (35, 42, 43). Pursuing our comparative approach of gal-9 and TCR signaling, we examined the relationships between the response to gal-9 and the status of Lck tyrosine phosphorylations in Jurkat cells. Following gal-9 treatment for various durations, protein extracts from Jurkat cells were analyzed by Western blot to detect the phosphorylation state of two conserved

## TCR Complex Signaling and Galectin-9 in Human T Cells

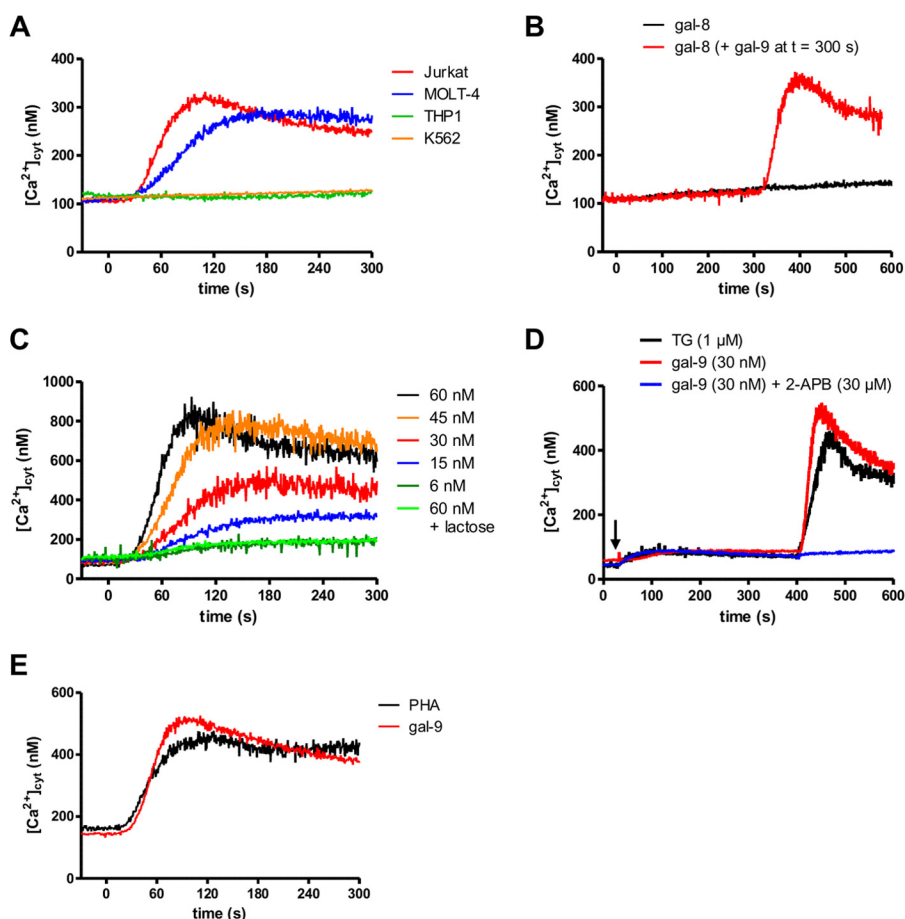


**FIGURE 2. Impact of gal-9 on  $[Ca^{2+}]_{cyt}$  in lymphoid T cells.** A, variations of cytosolic calcium concentrations following gal-9 addition to lymphoid and myeloid cells (Jurkat/MOLT-4 and THP1/K562, respectively).  $[Ca^{2+}]_{cyt}$  was assessed by Indo-1 fluorimetry in the presence of 1 mM extracellular  $CaCl_2$ . Gal-9 (30 nM final) was added at  $t = 0$  s. B, variations of  $[Ca^{2+}]_{cyt}$  in Jurkat cells treated with gal-8 (30 nM, added at  $t = 0$  s) alone (black line) or with gal-8 combined with secondary addition of gal-9 (30 nM, added at  $t = 300$  s) (red line). C, dose/effects relationships in Jurkat cells treated with increasing concentrations (6–60 nM) of gal-9.  $[Ca^{2+}]_{cyt}$  was recorded in the presence of 1 mM extracellular  $CaCl_2$ . The rise in  $[Ca^{2+}]_{cyt}$  was totally abolished by preincubation of gal-9 (30 nM) with a saturating concentration of lactose (5 mM). D, comparison of the impact of thapsigargin and gal-9 on calcium mobilization in Jurkat cells. Treatment of Jurkat cells with TG (1  $\mu$ M) or gal-9 (30 nM) with or without 2-aminoethoxydiphenyl borate (2-APB) (30  $\mu$ M) and in the absence of extracellular  $CaCl_2$  is indicated with a black arrow. Re-addition of  $CaCl_2$  was performed at  $t = 400$  s. E, comparison of the impact of PHA and gal-9 on calcium mobilization in Jurkat cells. Variations of  $[Ca^{2+}]_{cyt}$  in Jurkat cells were treated with gal-9 (30 nM) or PHA (10  $\mu$ g/ml) in the presence of 1 mM extracellular  $CaCl_2$ . All the experiments depicted in this figure are representative of at least two similar independent experiments.

tyrosine residues, Tyr-505 and Tyr-394, which are intramolecular regulators of Lck. As reported previously, a substantial fraction of Lck was already phosphorylated on its activatory (Tyr-394) and inhibitory (Tyr-505) tyrosines prior to any stimulation (Fig. 3C) (35, 42, 43). As also noted in previous studies, Tyr(P)-394 Lck, Tyr(P)-505 Lck, as well as the total Lck were distributed in two bands migrating at 59 and 55 kDa, respectively. In a previous publication (43), the slower migrating form was said to result from Ser-59 phosphorylation by ERK1/2. After 15 min of gal-9 treatment, a modest increase in the ratios of phosphorylated Lck to total Lck was detected for Tyr-394 and Tyr-505. These modifications were of larger amplitude for the slower migrating band (59 kDa) (Fig. 3C). Besides, treatment of Jurkat cells with the Lck inhibitor (200 nM) resulted in an almost complete suppression of Tyr-394 phosphorylation at baseline and under concomitant gal-9 stimulation (30 nM). A similar effect, although less intense, was observed for Tyr-505, although the amount of total Lck remained unchanged.

Next, we investigated whether Lck was required for the apoptotic pathway induced by gal-9. As shown in Fig. 3D, JCaM1.6

and WT Jurkat cells treated with gal-9 for 24 h were both sensitive to apoptosis. To confirm these results, WT Jurkat cells were treated for 8 h with gal-9 by itself or with concomitant application of the Lck inhibitor (200 nM or 1  $\mu$ M). Prior to these experiments, it was confirmed by Western blot analysis that the inhibitory effects of the Lck inhibitor were lasting for at least 8 h (Fig. 3E). As shown in Fig. 3F, apoptosis induction by gal-9 was not affected by the Lck inhibitor. Overall, these results supported the conclusion that a functional Lck molecule was required for calcium mobilization, but not for apoptosis, induced by gal-9 in Jurkat cells.

*TCR-CD3 Complex Is Required for Calcium Mobilization, but Not for Apoptosis, Induced by gal-9 in Jurkat Cells*—We postulated that some components of the TCR complex, normally acting upstream from the Lck kinase, were also required for the calcium mobilization induced by gal-9 in Jurkat cells. For this goal, we employed a panel of mutant Jurkat sublines with selective impairment of the CD3  $\zeta$ -chain (CD3 $\zeta^-$ ) or the TCR  $\beta$ -chain (J31.13) in addition to the JCaM1.6 subline (Lck $^-$ ), which has been previously introduced (29–31, 40). To

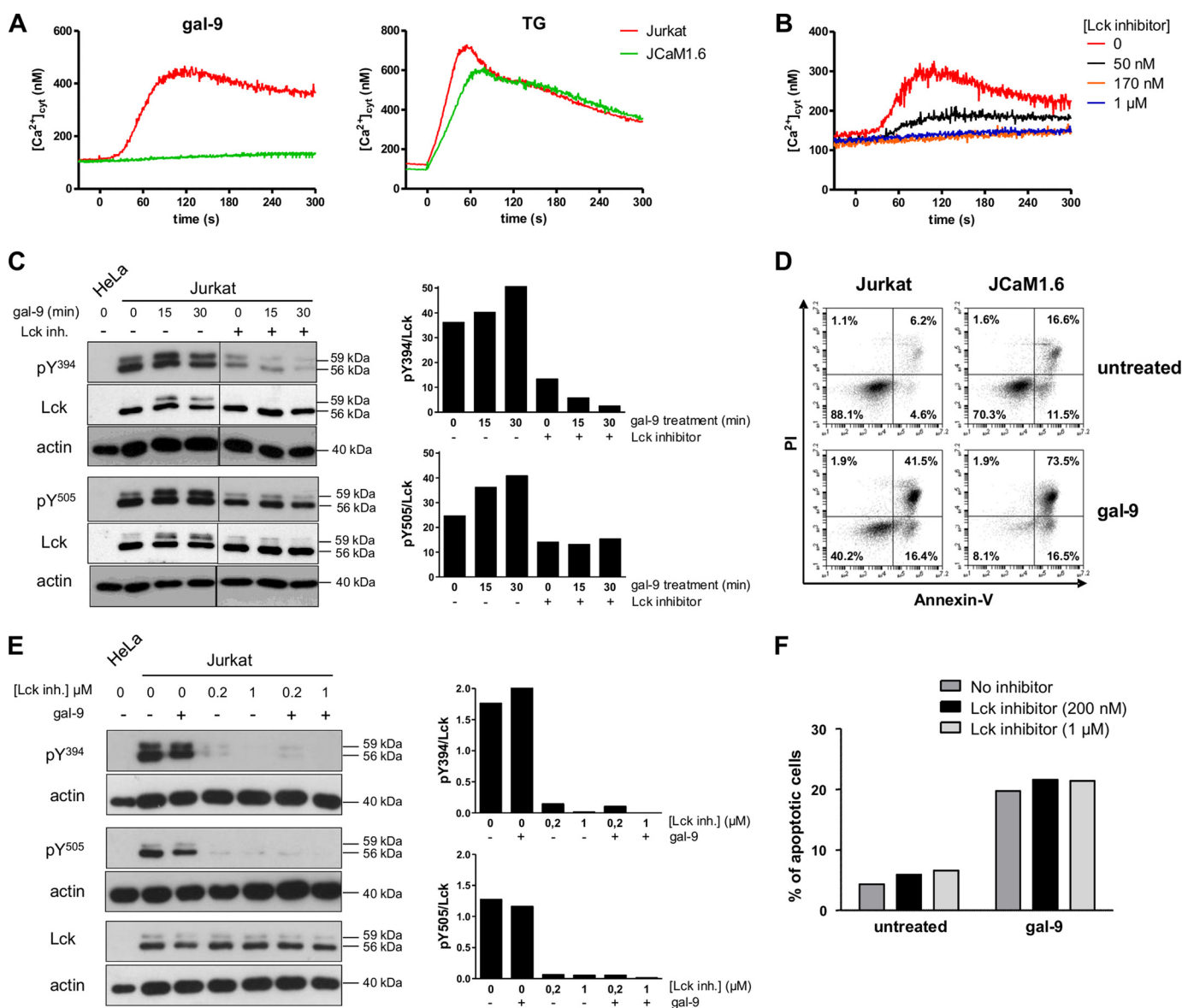


**FIGURE 3. Contribution of Lck to functional changes induced by gal-9 in Jurkat cells.** *A*, variations of  $[Ca^{2+}]_{\text{cyt}}$  in Jurkat and JCaM1.6 cells treated with gal-9 (30 nM) or TG (1  $\mu$ M) at  $t = 0$  s in the presence of 1 mM extracellular  $CaCl_2$ . Data presented here are representative of three similar independent experiments. *B*, impact of the Lck inhibitor (A-770041) on calcium mobilization induced by gal-9. Jurkat cells were preincubated or not with the Lck inhibitor (50 nM, 170 nM, or 1  $\mu$ M) for 30 min before gal-9 addition (30 nM) at  $t = 0$  s.  $[Ca^{2+}]_{\text{cyt}}$  was recorded in the presence of 1 mM extracellular  $CaCl_2$ . *C*, impact of gal-9 and Lck inhibitor on tyrosine phosphorylation of Lck in Jurkat cells (short term treatment). Jurkat cells serum-starved overnight were subjected to treatment with gal-9 (30 nM), with or without prior incubation with the Lck inhibitor (200 nM). After gal-9 treatment (15 or 30 min), protein extracts were analyzed by Western blot against the two phosphorylated forms of Lck (Tyr(P)-394 and Tyr(P)-505) or the total protein (Lck). As explained under "Experimental Procedures," to detect the phosphorylated form of Tyr-394 (Tyr(P)-394) we used an antibody raised against the phosphorylated form of the equivalent site in Src, Tyr-416. The histograms represent the ratio Tyr(P)-Lck/total Lck for the two tyrosines, which was estimated from the densitometry of the specific bands. Protein extracts from HeLa cells were used as negative controls for Lck expression. *D*, comparison of apoptosis induction by gal-9 in Jurkat and JCaM1.6 cells. After treatment with gal-9 (30 nM) for 24 h, cells were stained with annexin-V/PI and analyzed by flow cytometry. Plots are representative of four independent experiments. *E* and *F*, impact of gal-9 and Lck inhibitor on tyrosine phosphorylation of Lck and apoptosis in Jurkat cells (long term treatment). Jurkat cells serum-starved overnight were preincubated or not with the Lck inhibitor (200 nM or 1  $\mu$ M) before gal-9 treatment (30 nM) for 8 h. Then the sustained effect of the Lck inhibitor on Jurkat cells was analyzed by Western blot (*E*) as in *C*. gal-9-induced apoptosis was also analyzed (*F*) by annexin-V/PI staining.

make sure that the functional alterations observed in these cells were not related to other undeclared defects of the cell signaling machinery, we resorted to back-in clones. These clones were mutant cells where the expression of the WT protein had been restored by stable transfection of an exogenous gene. They were named JCaM1.6/Lck<sup>+</sup>, CD3 $\zeta$ <sup>+</sup>, and 31.13/TCR $\beta$ <sup>+</sup>, respectively. Short tandem repeat (STR) genotyping was performed to confirm

that all these cells (mutant sublines and back-ins) were derived from the same parental Jurkat cell line (Table 1 and Fig. 4A).

All WT Jurkat and derivative sublines were analyzed for Lck and CD3 $\zeta$  chain expression by Western blot (Fig. 4B). As expected, the Lck protein was absent in the JCaM1.6 subline, whereas its expression was restored in JCaM1.6/Lck<sup>+</sup> cells. The other sublines expressed similar levels of Lck. We observed a

**TABLE 1**  
STR genotyping of WT Jurkat cells and derivative sublines

Loci with alleles shared by all cell lines are highlighted in bold.

Cell line	D5S818	D7S820	D13S317	D16S539	Amelogenin	CSF1PO	THO1	TPOX	vWA
<b>STR data provided by the ATCC</b>									
Jurkat WT <sup>a</sup>	9	8,12	8,12	11	X,Y	11,12	<b>6,9,3</b>	<b>8,10</b>	18
JCaM1.6 <sup>b</sup>	9	8,10	8,12	10,11	X,Y	11	<b>6,9,3</b>	<b>8,10</b>	18,19
<b>STR data obtained in our laboratory</b>									
Jurkat WT	9	8,10	8,12	11	X,Y	11,12	<b>6,9,3</b>	<b>8,10</b>	18
JCaM1.6	9	8,10	8,12	10,11	X,Y	11	<b>6,9,3</b>	<b>8,10</b>	18,19
JCaM1.6/Lck+	9	8,10	8,12	10,11	X,Y	11,12	<b>6,9,3</b>	<b>8,10</b>	18
CD3ζ <sup>-</sup>	9	8,9,3	7,11	11	X,Y	10,14	<b>6,9,3</b>	<b>8,10</b>	16,18
CD3ζ <sup>+</sup>	9	8,9,3	7,11	11	X	9,14	<b>6,9,3</b>	<b>8,10</b>	16,18
J31.13	9	8,10	8,11	11	X,Y	11,12	<b>6,9,3</b>	<b>8,10</b>	18
J31.13/TCRβ <sup>+</sup>	9	8,10	8,11	11	X	11,12	<b>6,9,3</b>	<b>8,10</b>	16,18

<sup>a</sup> ID in the ATCC catalog, TIB-152.

<sup>b</sup> ID in the ATCC catalog, CRL-2063.

lower expression of CD3ζ in the J31.13 cells, which is consistent with a previous report (31). We also confirmed the absence of the ζ-chain expression in the CD3ζ<sup>-</sup> subline and its re-introduction in the CD3ζ<sup>+</sup> subline under a form of higher molecular weight. The panel of Jurkat derivative sublines was also analyzed by flow cytometry for cell surface expression of the TCRβ chain and CD3 components (Fig. 4C). Because the Jurkat cells express the specific variable region 8 of the TCRβ chain, we used a specific TCRVβ8 antibody (32, 44). As expected, the J31.13 subline was negative for both TCRβ and CD3 expression. Restoration of TCRβ and CD3 expression was achieved in ~75% of the cells in the J31.13/TCRβ<sup>+</sup> subline. In the CD3ζ<sup>-</sup> subline, the CD3 surface expression was not totally negative, because we used an antibody that reacts with the ε-chain of CD3. As for the J31.13 cells, the TCR and CD3 components were in mutual dependence for their surface expression in CD3ζ<sup>+</sup> and CD3ζ<sup>-</sup> sublines. Indeed, the re-introduction of the ζ-chain in the CD3ζ<sup>-</sup> subline restored the expression of the TCRβ at the cell surface.

As shown previously for JCaM1.6 cells, calcium mobilization under gal-9 stimulation was totally abrogated in the other mutant Jurkat sublines (J31.13 and CD3ζ<sup>-</sup>), indicating that the integrity of the TCR-CD3 complex was required for this process (Fig. 5A). TG treatment was used to verify that the mutant sublines were not deficient in other segments of the calcium signaling machinery. In addition, we could show that calcium mobilization induced by gal-9 or PHA was restored by re-introduction of the WT Lck, CD3ζ, or TCRβ proteins in the corresponding mutant cells. This was a formal proof that these molecules play a critical role in the short term calcium mobilization induced by gal-9 in Jurkat cells. On the contrary, when treated with gal-9 on a longer term, a large fraction of cells was undergoing apoptosis, in each type of mutant subline, exactly like for the WT Jurkat (Fig. 5, B and C). These results lead us to the conclusion that, in addition to the Lck kinase, proximal elements of the TCR complex were required in Jurkat cells for gal-9-induced calcium mobilization but not for apoptosis induction.

*Gal-9 Induces IL-2 and IFNγ Production in Jurkat and Peripheral T Cells*—The signaling events initiated at the TCR upon antigen stimulation in normal T cells ultimately lead to IL-2 production, which is essential for T cell proliferation and function. We investigated whether calcium mobilization triggered by gal-9 resulted in up-regulation of IL-2 production by Jurkat cells. In a first experiment, Jurkat and JCaM1.6 cells were

stimulated either with gal-9 or with a combination of anti-CD3 and -CD28 antibodies for 3 h. IL-2 mRNA expression was then analyzed by quantitative real time PCR (RT-qPCR). A substantial increase in the amount of IL-2 transcripts was observed in Jurkat cells under treatment with gal-9, although it was weaker than under the CD3/CD28 stimulation (Fig. 6A, *upper histogram*). In JCaM1.6 cells, the fold change for IL-2 mRNA was significantly reduced compared with WT Jurkat cells after gal-9 treatment. Up-regulation of IL-2 gene expression was sustained for at least 8 h in Jurkat cells, whereas in JCaM1.6 cells, IL-2 mRNA levels at 8 h was comparable with that of untreated cells (data not shown). The same experiment was performed with J31.13 cells, and the results were similar; the IL-2 mRNA expression was significantly reduced when cells were defective for TCR and CD3 expression (Fig. 6A, *bottom histogram*). In another experiment, the extracellular release of IL-2 was assessed by ELISA using Jurkat and JCaM1.6 cells stimulated with gal-9 (30 nM) or PHA (10 μg/ml) for 18 h (Fig. 6B). As expected, PHA stimulation led to an abundant IL-2 secretion by Jurkat cells, although a very low amount of IL-2 protein was detected in the supernatant of Lck-deficient JCaM1.6 cells. Although gal-9 stimulation in Jurkat cells induced a much lower production of IL-2 than PHA, notwithstanding the concentration differences (30 nM, *i.e.* 1 and 10 μg/ml respectively), there was a marked difference with JCaM1.6 cells, which were completely unable to produce noticeable IL-2 in response to gal-9.

In the next stages of our study, we wanted to test whether the observations made in Jurkat T cells were extensive to peripheral T cells from human donors. A preliminary step for this part of our investigations was to confirm the data reported by Gooden *et al.* (14) about the impact of gal-9 on peripheral T cells from healthy donors. Using human PBMCs, they reported a bimodal response to exogenous gal-9 with early apoptosis of a fraction of T cells followed by an antigen-independent activation of the remaining T cells, especially among CD4<sup>+</sup> T cells (14). To confirm these results, we treated freshly isolated PBMCs for 5 days with gal-9 (30 nM) or with gal-9 preincubated with a saturating concentration of lactose (5 mM). On day 5, CD3<sup>+</sup> cells were subjected to an intracellular staining assay to monitor the production of Th1 cytokines, IL-2 and IFNγ. Following gal-9 treatment, we observed an increase in the number of IL-2<sup>+</sup> and IFNγ<sup>+</sup> CD3<sup>+</sup> T cells, compared with untreated cells (Fig. 6, C and D). This T cell response, which was abrogated in the presence of lactose, was con-



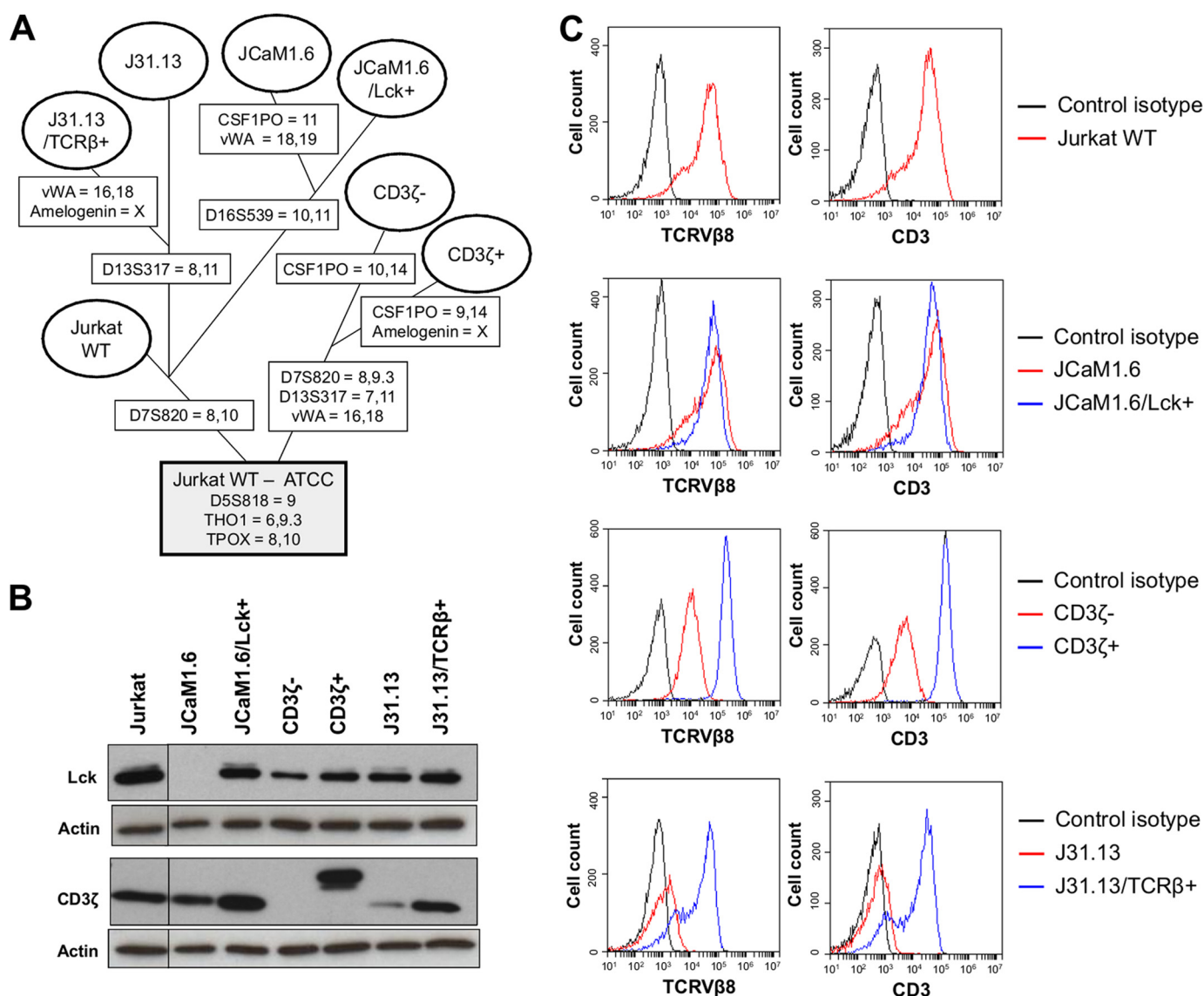


**FIGURE 4. Characterization of derivative Jurkat sublines.** *A*, tentative phylogenetic tree of the WT and derivative Jurkat sublines (mutants and back-clones). As shown in Table 1, three loci, *D5S818*, *THO1*, and *TPOX*, contain the same alleles in our WT Jurkat cells and the six derivative sublines. They are consistent with the ATCC official genotype of WT Jurkat cells. The evidence that all our Jurkat sublines are indeed derived from the same parental clone is strengthened by the similarity of many other alleles shared by at least two cell lines. It is worth noting that because Jurkat cells are deficient in mismatch repair due to a mutation in *MSH2* (62), the probability that insertion/deletion of tetranucleotide repeats in the STR markers arises during replication is higher than in normal cells. Loci-containing alleles not consistent with the ATCC official genotype are mentioned in boxes superimposed on the branches of the tree leading to the corresponding cell lines. Although purchased from the ATCC, our WT Jurkat cells carry one distinct allele at *D7S820*. The same allele is shared by J31.13, J31.13/TCRβ<sup>+</sup>, JCaM1.6, and JCaM1.6/Lck<sup>+</sup> cells. CD3ζ<sup>-</sup> is divergent from WT Jurkat and the other derivative sublines, J31.13 and JCaM1.6, at *D7S820*, *D13S317*, *CSF1PO*, and *vWA*. JCaM1.6 and J31.13 diverge from WT Jurkat at three (*D16S539*, *CSF1PO*, and *vWA*) and one locus (*D13S317*), respectively. This separation of J31.13 and JCaM1.6 on the one hand and CD3ζ<sup>-</sup> on the other hand is consistent with their distinctive historic features. JCaM1.6 and J31.13 were obtained much earlier by chemical and radiological somatic mutagenesis, respectively. They were reported in 1987. In contrast, CD3ζ<sup>-</sup> was obtained much more recently by stable transfection of an shRNA and was reported in 2012. *B*, Western blot analysis of Lck and CD3ζ expression in the different Jurkat derivative sublines. Actin protein levels were used as loading controls. *C*, cell surface expression of TCRβ8 and CD3 assessed by flow cytometry analysis in the different Jurkat derivative sublines. The black curves represent the cell surface staining with the control isotype, and the red and blue curves represent the staining of indicated cells with the TCRβ8 (left panel) or CD3 antibody (right panel). Data plots are representative of two independent experiments.

sistent with the notion of an antigen-independent activation of peripheral T cells by exogenous gal-9.

**Gal-9-induced Calcium Mobilization and Cytokine Production, but Not Apoptosis, Are Dependent on Lck in Peripheral CD4<sup>+</sup> T Cells**—Then, using PBMCs, we analyzed the contribution of Lck to the two faces of T cell response to gal-9, apoptosis and activation. Because activated human T cells have been reported to be more sensitive to gal-9 treatment than resting T cells, PBMCs were stimulated or not with anti-CD3 and anti-

CD28 antibodies for 48 h prior to gal-9 treatment (27). Then they were incubated with gal-9 (30 nM) that had been preincubated or not with lactose. After 24 h of incubation, treated PBMCs were subjected to flow cytometry analysis focused on CD4 expression and apoptosis detection. As shown in Fig. 7A, gal-9 significantly increased the frequency of annexin-V-positive CD4<sup>+</sup> T cells, either unstimulated or stimulated. This gal-9-induced apoptosis was almost completely suppressed by addition of lactose. In contrast, when PBMCs were incubated

## TCR Complex Signaling and Galectin-9 in Human T Cells

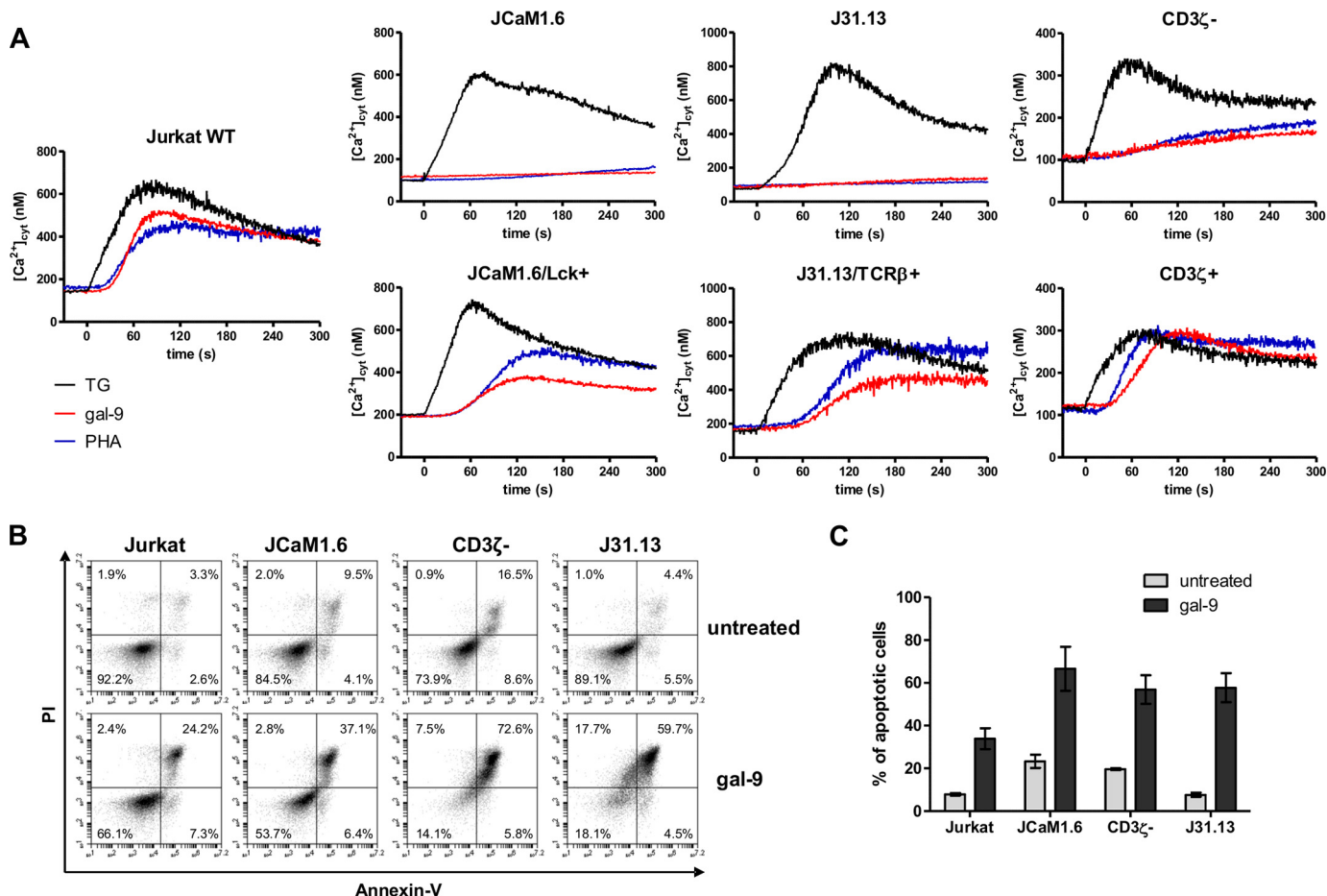


**FIGURE 5. Contribution of the TCR-CD3 complex to gal-9-induced modifications in Jurkat cells.** *A*, variations of  $[Ca^{2+}]_{cyt}$  in WT Jurkat and derivative sublines under stimulation by gal-9 (30 nM), PHA (10  $\mu$ g/ml), or TG (1  $\mu$ M) at  $t = 0$  s. *Graphs* presented here are representative of at least two similar experiments. *B* and *C*, apoptosis assay in the mutant defective sublines following 24 h of gal-9 treatment (30 nM). Flow cytometry plots (*B*) for annexin-V/PI staining in each cell line are representative of at least three independent experiments. Means  $\pm$  S.E. of annexin-V-positive cells (*C*) are not statistically different between cell lines, as assessed by two-way ANOVA.

with the Lck inhibitor prior to gal-9 treatment, the rate of CD4<sup>+</sup> T cell apoptosis was not modified (Fig. 7*B*). These results confirmed the data obtained with Jurkat cells; Lck signaling pathway is not involved in gal-9-induced apoptosis in T cells. To monitor the calcium mobilization induced by gal-9 in CD4<sup>+</sup> T cells, we used resting PBMCs loaded with Fluo4-AM and stained for CD4 expression before flow cytometry analysis. In this experiment, we used a higher concentration of gal-9 (120 nM) to stimulate the cells, for better detection and reading of fluorescence modifications on the flow cytometer. As in Jurkat cells, an increase in  $[Ca^{2+}]_{cyt}$  was induced by gal-9 and blocked by prior incubation with increasing concentrations of the Lck inhibitor (0.01 to 2  $\mu$ M) (Fig. 7, *C* and *D*). Finally, we investigated the impact of gal-9 on IL-2 and IFN $\gamma$  expression by CD4<sup>+</sup> T cells and its dependence on Lck. After isolation of CD4<sup>+</sup> T cells by negative depletion, cells were preincubated or not with the Lck inhibitor prior to treatment with gal-9 (30 nM), anti-CD3 antibody, anti-CD28 antibody or different combinations for 6 h. Then the RNA was extracted, and the expression of cytokines was analyzed by RT-qPCR (Fig. 7*E*). Gal-9 had effects that were somehow parallel to those of the anti-CD3, although less intense. The impact of the anti-CD28 by itself was negligible on the amount of both IL-2 and IFN $\gamma$  transcripts. In contrast, both

gal-9 and the anti-CD3 by themselves were able to increase the expression of IFN $\gamma$  mRNA. When they were combined with the anti-CD28, the enhancement of IFN $\gamma$  mRNA response was very strong for CD3 and modest for gal-9. Both gal-9 and the anti-CD3 alone were unable to increase the expression of IL-2 mRNA. However, this effect was achieved when either gal-9 or the anti-CD3 was combined to the anti-CD28. Moreover, the chemical inhibition of Lck completely abolished the cytokine expression in this experiment. Overall, these results confirm that the Lck signaling is crucial for the antigen-independent activation induced by gal-9 in peripheral T cells.

### Discussion

The initial question addressed by this work was whether or not calcium mobilization was one necessary step toward apoptosis of human T cells treated with extracellular gal-9. A careful analysis of the signature of calcium mobilization induced by gal-9 in Jurkat cells led us to hypothesize that it was dependent on the Lck tyrosine kinase. Using an Lck mutant derivative of Jurkat cells (JCaM1.6) and a chemical inhibitor of Lck (A-770041), we could confirm this hypothesis in Jurkat cells, as well as in CD4<sup>+</sup> T cells from the peripheral blood. Conversely, we could show that a functional Lck and calcium mobilization

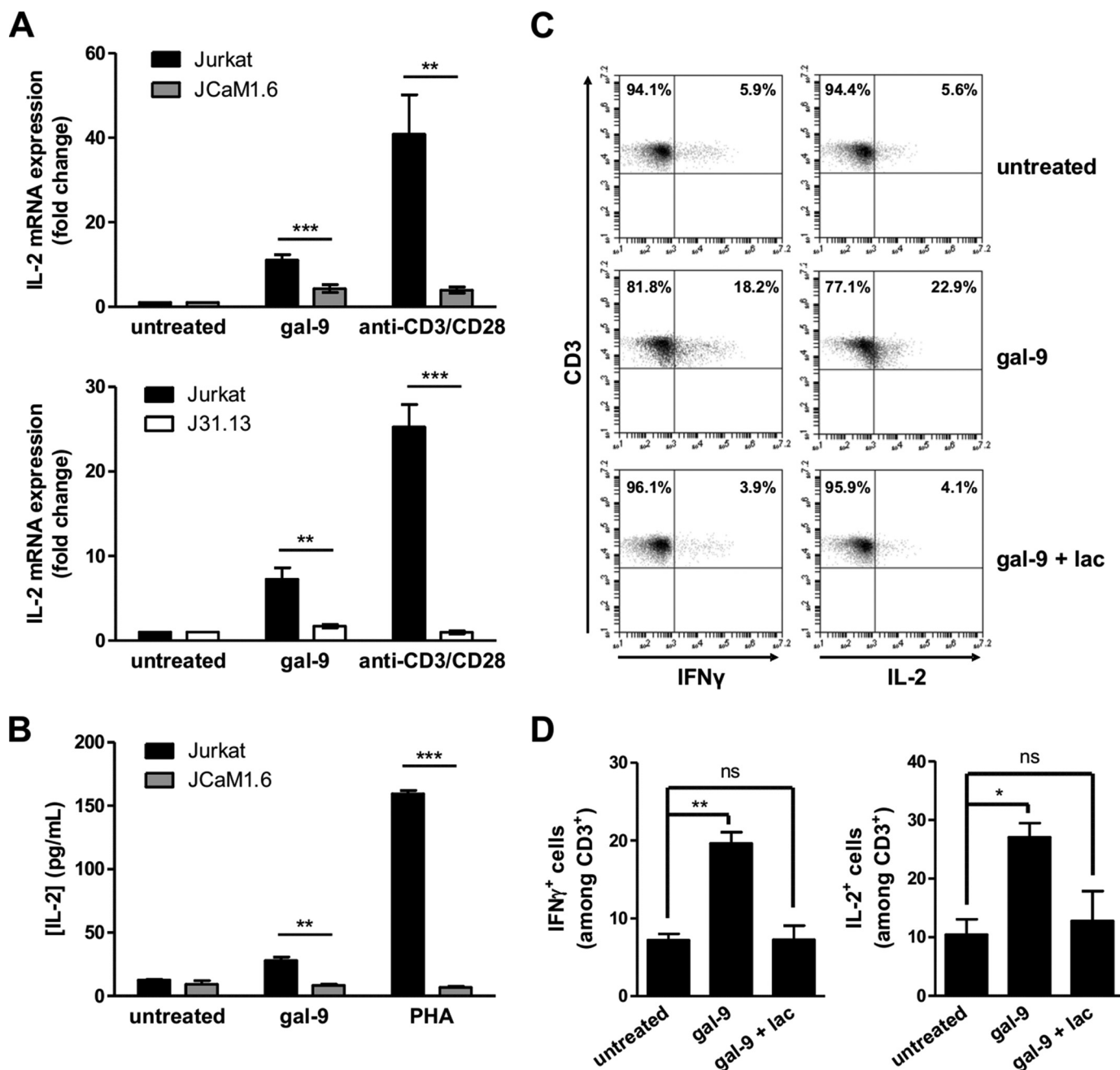


**FIGURE 6. Gal-9 induces IL-2 and IFN $\gamma$  production in Jurkat and peripheral T cells.** *A*, quantitative real time PCR determination of IL-2 mRNA expression in Jurkat, JCaM1.6 (upper histogram), or J31.13 (lower histogram) cells treated with either gal-9 (30 nM) or a combination of soluble anti-CD3 and anti-CD28 antibodies (1  $\mu$ g/ml) for 3 h. Data presented here correspond to the fold change defined as the ratio of target gene mRNA with that of untreated cells (the housekeeping gene TBP being used as an internal control). Means  $\pm$  S.E. of at least eight independent experiments are represented here. *B*, determination of IL-2 concentrations by ELISA in the culture media from Jurkat or JCaM1.6 cells treated for 24 h either with PHA (10  $\mu$ g/ml) or gal-9 (30 nM). Means  $\pm$  S.E. of three independent experiments are presented here. \*\*,  $p < 0.01$ ; \*\*\*,  $p < 0.001$ , two-tailed Student's  $t$  test with Welch's correction. *C* and *D*, PBMCs from healthy donors were treated with gal-9 (30 nM) or gal-9 preincubated with lactose (5 mM) for 5 days. Intracellular cytokine expression was assessed by flow cytometry immediately after PMA/ionomycin restimulation of PBMCs for 4 h as explained under "Experimental Procedures." After gating on CD3<sup>+</sup> T cells, IFN $\gamma$  (left panel) and IL-2 (right panel) expression were analyzed (*C*). The percentages of CD3<sup>+</sup> IL-2<sup>+</sup> and CD3<sup>+</sup> IFN $\gamma$ <sup>+</sup> cells are represented as means  $\pm$  S.E. of three independent experiments with different donors (*D*). \*,  $p < 0.05$ ; \*\*,  $p < 0.01$ , one-way ANOVA followed by Dunnett's post hoc test. *ns*, not significant.

were not required for apoptosis induction. We then addressed the question of whether components of the TCR-CD3 complex usually acting upstream from Lck were required for calcium mobilization induced by gal-9. Experiments realized with additional mutant Jurkat derivative sublines (CD3 $\zeta$ <sup>-</sup> and J31.13), and their corresponding back-in clones showed that CD3 $\zeta$  and TCR $\beta$  expression were dispensable for apoptosis induction,

although they were required for calcium mobilization. This led us to the idea that calcium mobilization induced by gal-9 might be part of a broader response reminiscent of antigen-dependent activation of T cells, involving Lck and maybe other components of the TCR complex. This latter hypothesis was confirmed to a large extent by the experiments reported in Fig. 7. These experiments have shown that gal-9 induces expression of

## TCR Complex Signaling and Galectin-9 in Human T Cells

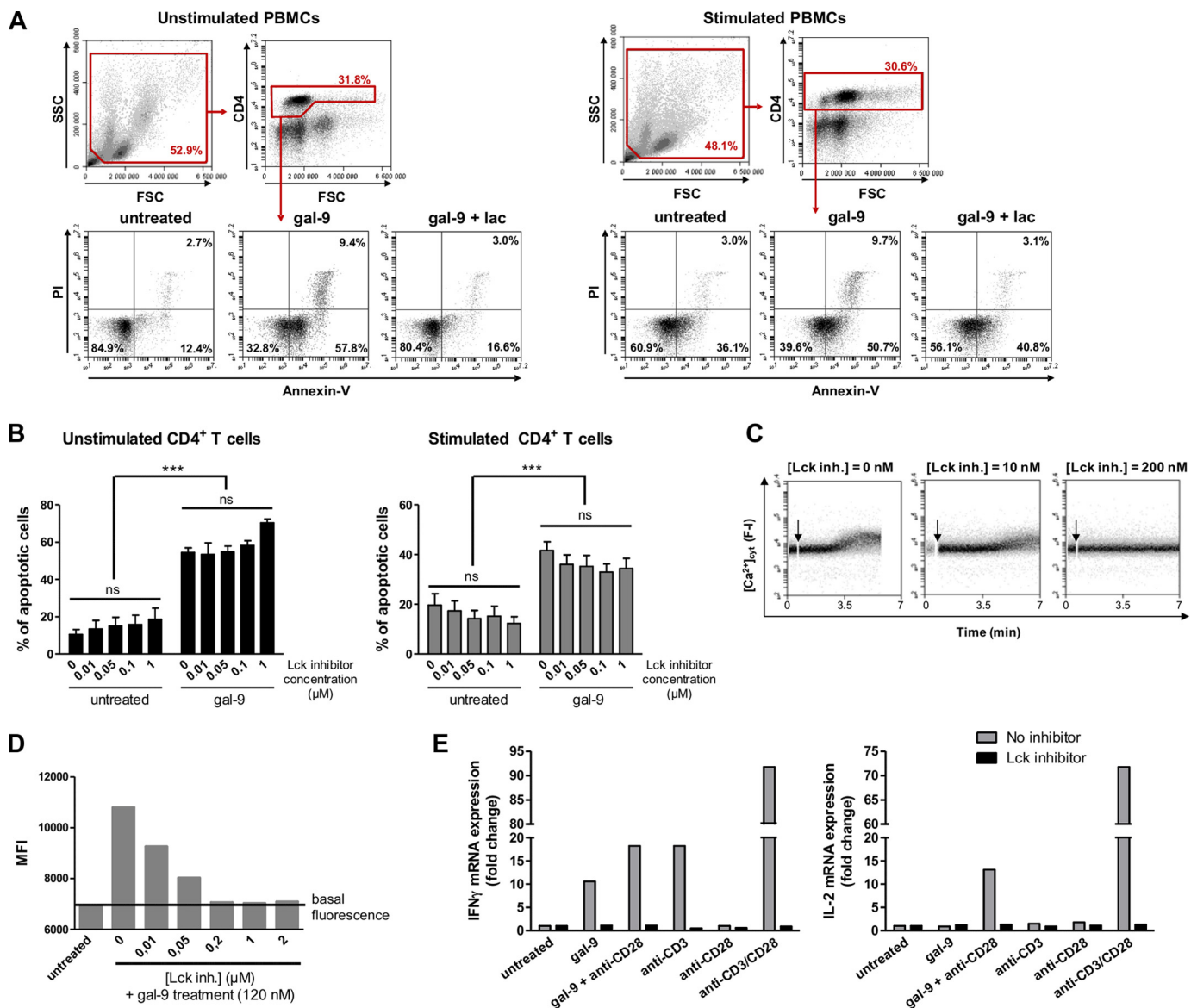


**FIGURE 7. Contribution of Lck to peripheral CD4<sup>+</sup> T cell response to gal-9.** A and B, PBMCs freshly isolated from blood were stimulated or not with anti-CD3 and anti-CD28 antibodies for 48 h. A, resting or activated PBMCs were preincubated or not with lactose (5 mM) prior to gal-9 treatment (30 nM) for 24 h. The percentage of apoptotic cells was determined by flow cytometry (annexin-V/PI staining) after gating on the CD4<sup>+</sup> population. Flow cytometry plots are representative of four independent experiments realized with different healthy donors. B, impact of the Lck inhibitor on gal-9-induced apoptosis in CD4<sup>+</sup> T cells. Resting or activated PBMCs were preincubated or not with the Lck inhibitor (0.01 to 1 μM) for 1 h before addition of gal-9 (30 nM) and incubation for 24 h. The percentages of apoptotic cells were determined as in A, taking account of all annexin-V-positive cells. Histograms represent means ± S.E. of three independent experiments with different donors. Statistical analyses using two-way ANOVA revealed no impact of the Lck inhibitor on the rate of apoptosis within the gal-9-untreated or gal-9-treated groups and a strong impact of gal-9 regardless of the presence or absence of the Lck inhibitor. \*\*\*, *p* < 0.001. ns, not significant. C and D, gal-9 induced calcium mobilization in peripheral CD4<sup>+</sup> T cells, which was blocked by Lck inhibition. Resting PBMCs were preincubated with Fluo4-AM (1 μM) for 45 min at room temperature. After washing and CD4 staining, cells were treated or not with the Lck inhibitor (0–2 μM) for 30 min before starting gal-9 stimulation (120 nM). C, fluorescence intensity (F-I; proportional to [Ca<sup>2+</sup>]<sub>cyt</sub>) continuous recording by flow cytometry after gal-9 addition (arrow). Plots are representative of [Ca<sup>2+</sup>]<sub>cyt</sub> variations in CD4<sup>+</sup> T cells in two independent experiments. D, mean fluorescence intensity (MFI) recorded in CD4<sup>+</sup> T cells measured on the different plots as in C, with the flow cytometer software. E, gal-9 induction of IL-2 and IFN $\gamma$  transcription and the impact of the Lck inhibitor. CD4<sup>+</sup> T cells isolated from resting PBMCs were preincubated or not with the Lck inhibitor (500 nM) for 1 h before treatment with gal-9 (30 nM) or the combination of anti-CD3 and anti-CD28 antibodies (1 μg/ml) for 6 h. IL-2 and IFN $\gamma$  mRNA expression were determined by quantitative real time PCR. Data presented here correspond to the fold change defined as the ratio of target gene mRNA with that of untreated cells (the housekeeping gene TBP was used as an internal control). These results are representative of two independent experiments.

Th1 cytokines, IL-2 and IFN $\gamma$ , in Jurkat cells, as well as in peripheral CD4<sup>+</sup> T cells in an Lck-dependent manner.

It is noteworthy that we provide the first confirmation of the observations reported by Gooden *et al.* (14) showing that some T cells treated with gal-9 and surviving early apoptosis (days 2 or 3) undergo activation, some of them acquiring a CD4<sup>+</sup> Th1 phenotype (days 6 or 7). However, we have been able to go

much further by demonstrating the essential role of Lck and the TCR-CD3 complex in this process. One may wonder how to reconcile these findings with the notion of an overall immunosuppressive action of gal-9 in intact organisms. This notion is based not only on experimental data from murine systems but also on observations made in human pathological conditions (9–12). We and others have previously reported data suggest-

ing a predominant immunosuppressive action of gal-9 in diseases like chronic active hepatitis or nasopharyngeal carcinomas related to the Epstein-Barr virus (16, 45–47). We believe that the activation of some CD4<sup>+</sup> Th1 cells by gal-9 is not likely to mitigate its overall immunosuppressive action for at least two reasons. First, the spread of T cells activated by gal-9 is probably not adequately focused on cells infected by pathogens. Second, diffuse IL-2 release by conventional T cells might contribute to the expansion of T regs (48).

Although we obtained compelling evidence of the participation of Lck in gal-9 signaling, we have observed only modest changes induced by gal-9 in the phosphorylation status of Lck in Jurkat cells (Fig. 3 and data not shown). As mentioned previously, this is consistent with previous reports about the contribution of Lck in TCR activation and signaling. Indeed, several investigators using cell lines or fresh peripheral T cells have observed only small changes in the phosphorylation status of Lck under TCR stimulation (35, 42, 43, 49). Moreover, the same authors have emphasized the fact that a baseline constitutive phosphorylation of Lck on Tyr-394 was required for efficient TCR signaling. Again, a similar trend is apparent regarding the response to gal-9 stimulation. Pretreatment of Jurkat cells with the Lck inhibitor, which suppresses Lck phosphorylation on Tyr-394 (and to a lesser extent on Tyr-505, Fig. 3C), also abrogates calcium mobilization following gal-9 stimulation. As for TCR signaling, we suspect that in addition to the basal constitutive state of Lck phosphorylation, its relocalization to distinct molecular complexes is very important for its contribution to gal-9 signaling (49).

One obvious question is which types of molecular interactions and events connect Lck activity to gal-9 binding on the plasma membrane of T cells. A few publications have reported direct or indirect interactions of Tim-3 with Lck or Fyn (50, 51). One of these publications based on murine cells has reported inhibition of Lck activity by the binding of exogenous gal-9 to Tim-3 (50). These findings are not relevant to our study because it is obvious that in Jurkat cells Lck was involved in the response to gal-9 in the absence of Tim-3 (see Fig. 1D). In contrast, data presented in Fig. 5 strongly suggest that members of the TCR-CD3 complex are required, upstream from Lck, to achieve calcium mobilization. Then the question arises of what makes a connection between gal-9 binding to the plasma membrane and changes of the TCR-CD3 complex. As mentioned previously, several surface proteins distinct from Tim-3 can bind gal-9 and have been proposed as candidate membrane receptors, especially CD44, CD137, and the enzyme disulfide isomerase (18, 23–25). Gal-9 can also bind surface glycolipids, for example the Forssman glycolipid (52). As far as we know, in the literature, there is no evidence of direct interactions of gal-9 with any member of the TCR-CD3 complex (53). One attractive hypothesis is that even in the absence of direct interactions, gal-9 might trigger activation of the TCR-CD3 complex by actions at the supra-molecular level, especially by bridging and inducing coalescence of otherwise distinct membrane micro- or nano-domains. Simultaneously gal-9 might favor the segregation of the TCR-CD3 complex from inhibitory molecules (54). This hypothesis is supported by two types of arguments. On the one hand, as a tandem repeat galectin bearing CRD of distinct specificity, gal-9 is expected to have specific bridging

functions. On the other hand, it is known that the formation of signaling TCR microclusters and later on of the immunological synapse requires spatial convergence of three types of elements as follows TCR components, Lck, and LAT proteins, which are initially bound to distinct vesicles and/or membrane nanodomains (49, 54). In future studies, it will be interesting to investigate the impact of gal-9 on the spatio-temporal organization of these three types of elements.

Other galectins are known to impact human T cells (36, 38, 53, 55). However, one needs to distinguish the influence of the endogenous galectins from the effects of extracellular galectins. In murine T cells, there is evidence that endogenous galectins, especially galectin-3, down-regulate TCR activation. It is proposed that interactions of galectins with branched surface ligands form a restrictive scaffold that limits TCR clustering required for the initiation of TCR signaling (56–58). In contrast, extracellular galectins, especially galectin-1, -3, or -8, have been reported to induce T cell activation in various experimental systems based on T cell lines or PBMCs (38, 53, 55). In sharp contrast with our findings about gal-9, several of these studies pointed out some kind of interdependence between T cell activation and apoptosis induction. For example, Brandt *et al.* (59) reported apoptosis induction in Jurkat cells treated with galectin-1 requiring an intact TCR-CD3 complex. It is important to notice that in the study of Brandt *et al.* (59), the concentrations of galectin-1 were in the range of 600–1800 nM instead of about 30 nM gal-9 in our own work. Nevertheless, these data suggest a lack of separation between apoptosis induction and T cell activation by galectin-1. In the same vein, Peng *et al.* (55) have reported induction of IFN $\gamma$  production in human T cell clones treated with galectin-3. Although a concentration of galectin-3 above 300 nM was required for this effect, when going above 750 nM, the production of IFN $\gamma$  was accompanied by an increasing rate of apoptosis (55). None of these studies dealing with T cell response to galectin-1, -3, and -8 have mentioned a role of Lck. Rather they have reported a role for CD45 (galectin-1 and galectin-3) or CD43 (galectin-1) (53, 58, 60, 61).

In conclusion, gal-9 induces apoptosis or activation in distinct subsets of human T cells, using two distinct signaling pathways. The pathway leading to CD4<sup>+</sup> Th1 activation involves the TCR-CD3 complex and Lck. According to currently published data, this pattern of T cell response seems to be unique to gal-9 and not applicable to galectin-1 or -3. One of our priorities will be to investigate the role of CD45, CD44, and CD43 upstream of gal-9-induced activation and/or apoptosis in human T cells.

---

*Acknowledgments*—We are indebted to Franck Gesbert and Richard Proust (Université Paris-Sud, France) for helpful discussions and their generous gift of CD3 $\zeta$ <sup>−</sup> and CD3 $\zeta$ <sup>+</sup> Jurkat sublines. We are grateful to Arthur Weiss (University of California at San Francisco) for the kind gift of JCaM1.6 and JCaM1.6/Lck<sup>+</sup> and Andres Alcover (Institut Pasteur, Paris, France) for J31.13 and J31.13/TCR<sup>+</sup>. We thank Nadira Delhem (Institut de Biologie de Lille, France), Georges Bismuth (Université Paris-Descartes, France), Jacques Bertoglio (Gustave Roussy, France), and Catherine Durieu (Gustave Roussy) for helpful discussions.

---

## References

- Boscher, C., Dennis, J. W., and Nabi, I. R. (2011) Glycosylation, galectins and cellular signaling. *Curr. Opin. Cell Biol.* **23**, 383–392
- Bacigalupo, M. L., Manzi, M., Rabinovich, G. A., and Troncoso, M. F. (2013) Hierarchical and selective roles of galectins in hepatocarcinogenesis, liver fibrosis and inflammation of hepatocellular carcinoma. *World J. Gastroenterol.* **19**, 8831–8849
- Heusschen, R., Griffioen, A. W., and Thijssen, V. L. (2013) Galectin-9 in tumor biology: a jack of multiple trades. *Biochim. Biophys. Acta* **1836**, 177–185
- Barjon, C., Niki, T., Vérillaud, B., Opolon, P., Bedossa, P., Hirashima, M., Blanchin, S., Wassef, M., Rosen, H. R., Jimenez, A. S., Wei, M., and Busson, P. (2012) A novel monoclonal antibody for detection of galectin-9 in tissue sections: application to human tissues infected by oncogenic viruses. *Infect. Agents Cancer* **7**, 16
- Keryer-Bibens, C., Pioche-Durieu, C., Villemant, C., Souquère, S., Nishi, N., Hirashima, M., Middeldorp, J., and Busson, P. (2006) Exosomes released by EBV-infected nasopharyngeal carcinoma cells convey the viral latent membrane protein 1 and the immunomodulatory protein galectin 9. *BMC Cancer* **6**, 283
- Mrizak, D., Martin, N., Barjon, C., Jimenez-Pailhes, A. S., Mustapha, R., Niki, T., Guigay, J., Pancré, V., de Launoit, Y., Busson, P., Moralès, O., and Delhem, N. (2015) Effect of nasopharyngeal carcinoma-derived exosomes on human regulatory T cells. *J. Natl. Cancer Inst.* **107**, 363
- Oomizu, S., Arikawa, T., Niki, T., Kadowaki, T., Ueno, M., Nishi, N., Yamauchi, A., Hattori, T., Masaki, T., and Hirashima, M. (2012) Cell surface galectin-9 expressing th cells regulate th17 and foxp3(+) Treg development by galectin-9 secretion. *PLoS One* **7**, e48574
- Jayaraman, P., Sada-Ovalle, I., Beladi, S., Anderson, A. C., Dardalhon, V., Hotta, C., Kuchroo, V. K., and Behar, S. M. (2010) Tim3 binding to galectin-9 stimulates antimicrobial immunity. *J. Exp. Med.* **207**, 2343–2354
- Reddy, P. B., Sehrawat, S., Suryawanshi, A., Rajasagi, N. K., Mulik, S., Hirashima, M., and Rouse, B. T. (2011) Influence of galectin-9/Tim-3 interaction on herpes simplex virus-1 latency. *J. Immunol.* **187**, 5745–5755
- Sharma, S., Sundararajan, A., Suryawanshi, A., Kumar, N., Veiga-Parga, T., Kuchroo, V. K., Thomas, P. G., Sangster, M. Y., and Rouse, B. T. (2011) T cell immunoglobulin and mucin protein-3 (Tim-3)/galectin-9 interaction regulates influenza A virus-specific humoral and CD8 T-cell responses. *Proc. Natl. Acad. Sci. U.S.A.* **108**, 19001–19006
- Wang, F., He, W., Zhou, H., Yuan, J., Wu, K., Xu, L., and Chen, Z. K. (2007) The Tim-3 ligand galectin-9 negatively regulates CD8<sup>+</sup> alloreactive T cell and prolongs survival of skin graft. *Cell. Immunol.* **250**, 68–74
- Moritoki, M., Kadowaki, T., Niki, T., Nakano, D., Soma, G., Mori, H., Kobara, H., Masaki, T., Kohno, M., and Hirashima, M. (2013) Galectin-9 ameliorates clinical severity of MRL/lpr lupus-prone mice by inducing plasma cell apoptosis independently of Tim-3. *PLoS One* **8**, e60807
- Anderson, A. C., Anderson, D. E., Bregoli, L., Hastings, W. D., Kassam, N., Lei, C., Chandwaskar, R., Karman, J., Su, E. W., Hirashima, M., Bruce, J. N., Kane, L. P., Kuchroo, V. K., and Hafler, D. A. (2007) Promotion of tissue inflammation by the immune receptor Tim-3 expressed on innate immune cells. *Science* **318**, 1141–1143
- Gooden, M. J., Wiersma, V. R., Samplonius, D. F., Gerssen, J., van Ginkel, R. J., Nijman, H. W., Hirashima, M., Niki, T., Eggleton, P., Helfrich, W., and Bremer, E. (2013) Galectin-9 activates and expands human T-helper 1 cells. *PLoS One* **8**, e65616
- Seki, M., Oomizu, S., Sakata, K. M., Sakata, A., Arikawa, T., Watanabe, K., Ito, K., Takeshita, K., Niki, T., Saita, N., Nishi, N., Yamauchi, A., Katoh, S., Matsukawa, A., Kuchroo, V., and Hirashima, M. (2008) Galectin-9 suppresses the generation of Th17, promotes the induction of regulatory T cells, and regulates experimental autoimmune arthritis. *Clin. Immunol.* **127**, 78–88
- Mengshol, J. A., Golden-Mason, L., Arikawa, T., Smith, M., Niki, T., McWilliams, R., Randall, J. A., McMahan, R., Zimmerman, M. A., Rangachari, M., Dobrinskikh, E., Busson, P., Polyak, S. J., Hirashima, M., and Rosen, H. R. (2010) A crucial role for Kupffer cell-derived galectin-9 in regulation of T cell immunity in hepatitis C infection. *PLoS One* **5**, e9504
- Kared, H., Fabre, T., Bédard, N., Bruneau, J., and Shoukry, N. H. (2013) Galectin-9 and IL-21 mediate cross-regulation between Th17 and Treg cells during acute hepatitis C. *PLoS Pathog* **9**, e1003422
- Wu, C., Thalhamer, T., Franca, R. F., Xiao, S., Wang, C., Hotta, C., Zhu, C., Hirashima, M., Anderson, A. C., and Kuchroo, V. K. (2014) Galectin-9-CD44 interaction enhances stability and function of adaptive regulatory T cells. *Immunity* **41**, 270–282
- Zhu, C., Anderson, A. C., Schubart, A., Xiong, H., Imitola, J., Khoury, S. J., Zheng, X. X., Strom, T. B., and Kuchroo, V. K. (2005) The Tim-3 ligand galectin-9 negatively regulates T helper type 1 immunity. *Nat. Immunol.* **6**, 1245–1252
- Su, E. W., Bi, S., and Kane, L. P. (2011) Galectin-9 regulates T helper cell function independently of Tim-3. *Glycobiology* **21**, 1258–1265
- Leitner, J., Rieger, A., Pickl, W. F., Zlabinger, G., Grabmeier-Pfistershammer, K., and Steinberger, P. (2013) TIM-3 does not act as a receptor for galectin-9. *PLoS Pathog* **9**, e1003253
- Golden-Mason, L., McMahan, R. H., Strong, M., Reisdorph, R., Mahaffey, S., Palmer, B. E., Cheng, L., Kulesza, C., Hirashima, M., Niki, T., and Rosen, H. R. (2013) Galectin-9 functionally impairs natural killer cells in humans and mice. *J. Virol.* **87**, 4835–4845
- Bi, S., Hong, P. W., Lee, B., and Baum, L. G. (2011) Galectin-9 binding to cell surface protein disulfide isomerase regulates the redox environment to enhance T-cell migration and HIV entry. *Proc. Natl. Acad. Sci. U.S.A.* **108**, 10650–10655
- Tanikawa, R., Tanikawa, T., Hirashima, M., Yamauchi, A., and Tanaka, Y. (2010) Galectin-9 induces osteoblast differentiation through the CD44/Smad signaling pathway. *Biochem. Biophys. Res. Commun.* **394**, 317–322
- Madireddi, S., Eun, S. Y., Lee, S. W., Nemčovičová, I., Mehta, A. K., Zajonc, D. M., Nishi, N., Niki, T., Hirashima, M., and Croft, M. (2014) Galectin-9 controls the therapeutic activity of 4–1BB-targeting antibodies. *J. Exp. Med.* **211**, 1433–1448
- Lu, L. H., Nakagawa, R., Kashio, Y., Ito, A., Shoji, H., Nishi, N., Hirashima, M., Yamauchi, A., and Nakamura, T. (2007) Characterization of galectin-9-induced death of Jurkat T cells. *J. Biochem.* **141**, 157–172
- Kashio, Y., Nakamura, K., Abedin, M. J., Seki, M., Nishi, N., Yoshida, N., Nakamura, T., and Hirashima, M. (2003) Galectin-9 induces apoptosis through the calcium-calpain-caspase-1 pathway. *J. Immunol.* **170**, 3631–3636
- Nishi, N., Itoh, A., Fujiyama, A., Yoshida, N., Araya, S., Hirashima, M., Shoji, H., and Nakamura, T. (2005) Development of highly stable galectins: truncation of the linker peptide confers protease-resistance on tandem repeat type galectins. *FEBS Lett.* **579**, 2058–2064
- Straus, D. B., and Weiss, A. (1992) Genetic evidence for the involvement of the lck tyrosine kinase in signal transduction through the T cell antigen receptor. *Cell* **70**, 585–593
- Proust, R., Bertoglio, J., and Gesbert, F. (2012) The adaptor protein SAP directly associates with CD3 $\zeta$  chain and regulates T cell receptor signaling. *PLoS One* **7**, e43200
- Alcover, A., Alberini, C., Acuto, O., Clayton, L. K., Transy, C., Spagnoli, G. C., Moingeon, P., Lopez, P., and Reinherz, E. L. (1988) Interdependence of CD3-Ti and CD2 activation pathways in human T lymphocytes. *EMBO J.* **7**, 1973–1977
- Alcover, A., Mariuzza, R. A., Ermonval, M., and Acuto, O. (1990) Lysine 271 in the transmembrane domain of the T-cell antigen receptor  $\beta$  chain is necessary for its assembly with the CD3 complex but not for  $\alpha/\beta$  dimerization. *J. Biol. Chem.* **265**, 4131–4135
- Lequin, D., Fizazi, K., Toujani, S., Souquère, S., Mathieu, M. C., Hainaut, P., Bernheim, A., Praz, F., and Busson, P. (2007) Biological characterization of two xenografts derived from human CUPs (carcinomas of unknown primary). *BMC Cancer* **7**, 225
- Djillani, A., Nüsse, O., and Dellis, O. (2014) Characterization of novel store-operated calcium entry effectors. *Biochim. Biophys. Acta* **1843**, 2341–2347
- Nika, K., Soldani, C., Salek, M., Paster, W., Gray, A., Etzensperger, R., Fugger, L., Polzella, P., Cerundolo, V., Dushek, O., Höfer, T., Viola, A., and Acuto, O. (2010) Constitutively active Lck kinase in T cells drives antigen receptor signal transduction. *Immunity* **32**, 766–777
- Bi, S., Earl, L. A., Jacobs, L., and Baum, L. G. (2008) Structural features of

- galectin-9 and galectin-1 that determine distinct T cell death pathways. *J. Biol. Chem.* **283**, 12248–12258
37. Wiersma, V. R., de Bruyn, M., van Ginkel, R. J., Sigar, E., Hirashima, M., Niki, T., Nishi, N., Samplonius, D. F., Helfrich, W., and Bremer, E. (2012) The glycan-binding protein galectin-9 has direct apoptotic activity toward melanoma cells. *J. Invest. Dermatol.* **132**, 2302–2305
  38. Tribulatti, M. V., Cattaneo, V., Hellman, U., Mucci, J., and Campetella, O. (2009) Galectin-8 provides costimulatory and proliferative signals to T lymphocytes. *J. Leukocyte Biol.* **86**, 371–380
  39. Altman, A., Coggeshall, K. M., and Mustelin, T. (1990) Molecular events mediating T cell activation. *Adv. Immunol.* **48**, 227–360
  40. Abraham, R. T., and Weiss, A. (2004) Jurkat T cells and development of the T-cell receptor signalling paradigm. *Nat. Rev. Immunol.* **4**, 301–308
  41. Stachlewitz, R. F., Hart, M. A., Bettencourt, B., Kebede, T., Schwartz, A., Ratnofsky, S. E., Calderwood, D. J., Waegell, W. O., and Hirst, G. C. (2005) A-770041, a novel and selective small-molecule inhibitor of Lck, prevents heart allograft rejection. *J. Pharmacol. Exp. Ther.* **315**, 36–41
  42. Paster, W., Paar, C., Eckerstorfer, P., Jakober, A., Drbal, K., Schutz, G. J., Sonnleitner, A., and Stockinger, H. (2009) Genetically encoded Förster resonance energy transfer sensors for the conformation of the Src family kinase Lck. *J. Immunol.* **182**, 2160–2167
  43. Dong, S., Corre, B., Nika, K., Pellegrini, S., and Michel, F. (2010) T cell receptor signal initiation induced by low-grade stimulation requires the cooperation of LAT in human T cells. *PLoS One* **5**, e15114
  44. Poppema, S., and Hepperle, B. (1991) Restricted V gene usage in T-cell lymphomas as detected by anti-T-cell receptor variable region reagents. *Am. J. Pathol.* **138**, 1479–1484
  45. Klibi, J., Niki, T., Riedel, A., Pioche-Durieu, C., Souquere, S., Rubinstein, E., Le Moulec, S., Moulec, S. L., Guigay, J., Hirashima, M., Guemira, F., Adhikary, D., Mautner, J., and Busson, P. (2009) Blood diffusion and Th1-suppressive effects of galectin-9-containing exosomes released by Epstein-Barr virus-infected nasopharyngeal carcinoma cells. *Blood* **113**, 1957–1966
  46. Barjon, C., Niki, T., Vérillaud, B., Opolon, P., Bedossa, P., Hirashima, M., Blanchin, S., Wassef, M., Rosen, H. R., Jimenez, A.-S., Wei, M., and Busson, P. (2012) A novel monoclonal antibody for detection of galectin-9 in tissue sections: application to human tissues infected by oncogenic viruses. *Infect. Agent. Cancer* **7**, 16
  47. Li, H., Wu, K., Tao, K., Chen, L., Zheng, Q., Lu, X., Liu, J., Shi, L., Liu, C., Wang, G., and Zou, W. (2012) Tim-3/galectin-9 signaling pathway mediates T-cell dysfunction and predicts poor prognosis in patients with hepatitis B virus-associated hepatocellular carcinoma. *Hepatology* **56**, 1342–1351
  48. Oomizu, S., Arikawa, T., Niki, T., Kadowaki, T., Ueno, M., Nishi, N., Yamachi, A., and Hirashima, M. (2012) Galectin-9 suppresses Th17 cell development in an IL-2-dependent but Tim-3-independent manner. *Clin. Immunol.* **143**, 51–58
  49. Soares, H., Henriques, R., Sachse, M., Ventimiglia, L., Alonso, M. A., Zimer, C., Thoulouze, M. I., and Alcover, A. (2013) Regulated vesicle fusion generates signaling nanoterritories that control T cell activation at the immunological synapse. *J. Exp. Med.* **210**, 2415–2433
  50. Rangachari, M., Zhu, C., Sakuishi, K., Xiao, S., Karman, J., Chen, A., Angin, M., Wakeham, A., Greenfield, E. A., Sobel, R. A., Okada, H., McKinnon, P. J., Mak, T. W., Addo, M. M., Anderson, A. C., and Kuchroo, V. K. (2012) Bat3 promotes T cell responses and autoimmunity by repressing Tim-3-mediated cell death and exhaustion. *Nat. Med.* **18**, 1394–1400
  51. Lee, J., Su, E. W., Zhu, C., Hainline, S., Phuah, J., Moroco, J. A., Smithgall, T. E., Kuchroo, V. K., and Kane, L. P. (2011) Phosphotyrosine-dependent coupling of Tim-3 to T-cell receptor signaling pathways. *Mol. Cell. Biol.* **31**, 3963–3974
  52. Hirabayashi, J., Hashidate, T., Arata, Y., Nishi, N., Nakamura, T., Hirashima, M., Urashima, T., Oka, T., Futai, M., Muller, W. E., Yagi, F., and Kasai, K. (2002) Oligosaccharide specificity of galectins: a search by frontal affinity chromatography. *Biochim. Biophys. Acta* **1572**, 232–254
  53. Walzel, H., Blach, M., Hirabayashi, J., Kasai, K. I., and Brock, J. (2000) Involvement of CD2 and CD3 in galectin-1 induced signaling in human Jurkat T-cells. *Glycobiology* **10**, 131–140
  54. Brownlie, R. J., and Zamoyska, R. (2013) T cell receptor signalling networks: branched, diversified and bounded. *Nat. Rev. Immunol.* **13**, 257–269
  55. Peng, W., Wang, H. Y., Miyahara, Y., Peng, G., and Wang, R. F. (2008) Tumor-associated galectin-3 modulates the function of tumor-reactive T cells. *Cancer Res.* **68**, 7228–7236
  56. Chen, I. J., Chen, H. L., and Demetriou, M. (2007) Lateral compartmentalization of T cell receptor versus CD45 by galectin-N-glycan binding and microfilaments coordinate basal and activation signaling. *J. Biol. Chem.* **282**, 35361–35372
  57. Demetriou, M., Granovsky, M., Quaggin, S., and Dennis, J. W. (2001) Negative regulation of T-cell activation and autoimmunity by Mgat5N-glycosylation. *Nature* **409**, 733–739
  58. Hsu, D. K., Chen, H. Y., and Liu, F. T. (2009) Galectin-3 regulates T-cell functions. *Immunol. Rev.* **230**, 114–127
  59. Brandt, B., Abou-Eladab, E. F., Tiedge, M., and Walzel, H. (2010) Role of the JNK/c-Jun/AP-1 signaling pathway in galectin-1-induced T-cell death. *Cell Death Dis.* **1**, e23
  60. Stillman, B. N., Hsu, D. K., Pang, M., Brewer, C. F., Johnson, P., Liu, F. T., and Baum, L. G. (2006) Galectin-3 and galectin-1 bind distinct cell surface glycoprotein receptors to induce T cell death. *J. Immunol.* **176**, 778–789
  61. Pace, K. E., Lee, C., Stewart, P. L., and Baum, L. G. (1999) Restricted receptor segregation into membrane microdomains occurs on human T cells during apoptosis induced by galectin-1. *J. Immunol.* **163**, 3801–3811
  62. Brimmell, M., Mendiola, R., Mangion, J., and Packham, G. (1998) BAX frameshift mutations in cell lines derived from human haemopoietic malignancies are associated with resistance to apoptosis and microsatellite instability. *Oncogene* **16**, 1803–1812